TU Delft

Delft University of Technology

Document Version
Final published version

Licence
CC BY

Citation (APA)
Burghardt, L., Poppema, D. W., Bénet, L., Erpicum, S., Wüthrich, D., & Klopries, E. M. (2026). A Multilaboratory Evaluation of Backwater Effects at Bridges Resulting from Diverse Floating Debris Compositions during the 2021 Flood Event in Europe. *Journal of Hydraulic Engineering, 152*(6), Article 04026038. https://doi.org/10.1061/JHEND8.HYENG-14517

Important note
To cite this publication, please use the final published version (if applicable).
Please check the document version above.

Copyright
In case the licence states “Dutch Copyright Act (Article 25fa)”, this publication was made available Green Open Access via the TU Delft Institutional Repository pursuant to Dutch Copyright Act (Article 25fa, the Taverne amendment). This provision does not affect copyright ownership.
Unless copyright is transferred by contract or statute, it remains with the copyright holder.

Sharing and reuse
Other than for strictly personal use, it is not permitted to download, forward or distribute the text or part of it, without the consent of the author(s) and/or copyright holder(s), unless the work is under an open content license such as Creative Commons.

Takedown policy
Please contact us and provide details if you believe this document breaches copyrights.
We will remove access to the work immediately and investigate your claim.

This work is downloaded from Delft University of Technology.

A Multilaboratory Evaluation of Backwater Effects at Bridges Resulting from Diverse Floating Debris Compositions during the 2021 Flood Event in Europe

Lisa Burghardt[1]; Daan Willem Poppema[2]; Loïc Bénet[3]; Sébastien Erpicum, M.ASCE[4]; Davide Wüthrich[5]; and Elena-Maria Klopries[6]

Abstract: The flood event of July 2021 in Western Europe was characterized by water levels far above the 100-year design flood and by billions of euros in damages. During the flood, voluminous debris accumulations of up to 4,000 m^3 occurred at various bridges, causing backwater rise and increased inundation depths. These accumulations contained large amounts of man-made materials, in particular cars, building rubble and household items in addition to driftwood. Therefore, a multilaboratory test series was conducted in this study, aiming to quantify the effect of debris composition and bridge design on backwater rise. Two model scales and seven different debris compositions were studied with the help of flume experiments, carried out in parallel in three laboratories in Belgium, Germany, and the Netherlands. Based on postflood field observations, man-made debris was represented by plates and cubes, mixed with logs. Results showed similar correlations between debris composition and backwater rise in all three laboratories. Compared to debris mixtures with only logs, an increasing volume fraction of plate-shaped objects increased backwater rise due to their higher interlocking nature, while an increasing share of cuboid objects generated less backwater rise. In all cases, backwater rise increased with increasing Froude numbers above 0.13 for constant debris volumes. In contrast, relative backwater rise decreased with increasing initial water level and for a higher bridge blockage ratio. The design of the bridge deck influenced both clogging behavior as well as backwater rise at the bridge, and closed handrails led to higher backwater rise compared to configurations with porous or no handrails. When comparing the results from all laboratories, only minor differences were observed, showing consistency in the methodology. Finally, this study presents a predictive equation to determine backwater rise at bridges in narrow river sections considering debris composition, bridge design and hydraulic conditions. **DOI: 10.1061/JHEND8.HYENG-14517**. *This work is made available under the terms of the Creative Commons Attribution 4.0 International license, https://creativecommons.org/licenses/by/4.0/.*

Author keywords: Bridge clogging; Debris accumulation; Bridge designs; Backwater rise; Flume experiments.

This work is made available under the terms of the Creative Commons Attribution 4.0 International license.

Introduction

In July 2021, flood events of catastrophic proportions occurred in Western Europe leading to over 200 casualties and billions of euros in damages in Belgium and Germany (Koks et al. 2022; Mohr et al. 2023). Parts of critical infrastructure, including utility networks, roads, and bridges, were severely damaged, hampering rescue measures (Lehmkuhl et al. 2022; Wüthrich et al. 2025). Bridges showed the presence of large floating debris accumulations, composed of large wood (LW) from trees as well as additional items of various anthropogenic components (Poppema et al. 2025), leading to increased water levels and larger inundation areas (Burghardt et al. 2024a; Landesamt für Umwelt Rheinland-Pfalz 2022). A combination of increased loads on bridges, caused by rising water levels, bridges overtopping, and debris accumulations led to widespread damages and to at least 45 bridge failures solely in Germany (Burghardt et al. 2024a). The collapse of an impounded bridge can further increase the damage potential by releasing flood waves of water and debris (Landesamt für Umwelt Rheinland-Pfalz 2022; Martín-Vide et al. 2023; Tubaldi et al. 2022). Further, channel widening, scour, and backward erosion were observed near bridges, with many showing signs of debris accumulations (Burghardt et al. 2024a; Lehmkuhl et al. 2022). Flood events in France, Italy, Switzerland, and Spain in the past two years also highlight the rising importance of debris accumulations during extreme flooding, especially in the context of undergoing climate change (Franca et al. 2024).

In recent years, the impact of debris accumulations at obstacles (e.g., bridges, racks, and culverts) has gained relevance in flood risk management. Previous research has studied various aspects including backwater rise, scour or blockage probability at single bridge piers without a deck (Cantero-Chinchilla et al. 2021; Innocenti et al. 2025; Schalko et al. 2019), various bridge deck

[1]Research Associate, Institute of Hydraulic Engineering and Water Resources Management, RWTH Aachen Univ., Aachen 52074, Germany (corresponding author). ORCID: https://orcid.org/0009-0004-4290-5788. Email: burghardt@iww.rwth-aachen.de

[2]Postdoc Researcher, Dept. of Hydraulic Engineering, Delft Univ. of Technology, Delft 2600 AA, Netherlands. ORCID: https://orcid.org/0000-0002-6142-3790. Email: d.w.poppema@tudelft.nl

[3]Engineer, SRP Ingénieur AG, Brig 3900, Switzerland; formerly, Hydraulics in Environmental and Civil Engineering, Liège Univ., Liège 4000, Belgium. Email: loicbenet@hotmail.com

[4]Associate Professor, Hydraulics in Environmental and Civil Engineering, Liège Univ., Liège 4000, Belgium. ORCID: https://orcid.org/0000-0002-7094-9604. Email: s.erpicum@uliege.be

[5]Assistant Professor, Dept. of Hydraulic Engineering, Delft Univ. of Technology, Delft 2600 AA, Netherlands. ORCID: https://orcid.org/0000-0003-1974-3560. Email: d.wuthrich@tudelft.nl

[6]Senior Scientific Staff, Institute of Hydraulic Engineering and Water Resources Management, RWTH Aachen Univ., Aachen 52074, Germany. ORCID: https://orcid.org/0000-0003-4752-6619. Email: klopries@iww.rwth-aachen.de

Note. This manuscript was submitted on February 11, 2025; approved on March 3, 2026; published online on August 5, 2026. Discussion period open until January 5, 2027; separate discussions must be submitted for individual papers. This paper is part of the ***Journal of Hydraulic Engineering***, ASCE, ISSN 0733-9429.

designs (Gschnitzer et al. 2017; Schmocker and Hager 2011), debris racks (Schmocker and Hager 2013; Schmocker and Weitbrecht 2013), culverts and inverted syphons (Ronckers et al. 2024), flexible barriers (Lambert et al. 2023; Piton et al. 2023), and weirs and spillways (Bénet et al. 2021; Furlan 2019; Schmocker et al. 2016), considering various flow conditions (Diehl 1997; Lange and Bezzola 2006), with movable and fixed beds (Piton et al. 2023; Schalko 2018). All of these studies used debris that simulated trees and occasionally fine organic materials. Schalko (2018) developed a design equation for normalized backwater rise of log accumulations at debris racks depending on the accumulation type factor f_A, the Froude number of the approach flow $Fr_0 = v_0/(gh_0)^{0.5}$ with the approach flow depth h_0, the initial flow velocity v_0 and the gravitational acceleration g, the solid large wood volume V_s, the flume width B, the log diameter d_L and the percentage of fine materials (FM), resulting in Eq. (1). The factor f_A depends on the formation of the accumulation, with predefined accumulations resulting in $f_A = 1$, as well as the river bed conditions with $f_A = 0.55$ for natural accumulations at fixed beds or $f_A = 0.3$ for natural accumulations at movable beds (Schalko 2018). The bulk factor a was defined as the ratio between loose large wood volume and solid large wood volume and was determined empirically as a function of the approach flow conditions with $a \approx 5–1.35Fr_0$ (Schalko 2018)

$$\frac{\Delta h}{h_0} = 5.4 f_A \frac{Fr_0\left(\frac{V_s}{Bd_L h_0}\right)^{\frac{1}{3}}(9FM+1)}{a} \quad (1)$$

However, the visible floating debris during the 2021 flood event showed a large share of man-made materials of various shapes and sizes, including building rubble, vehicles, and furniture (Erpicum et al. 2024; Poppema et al. 2025). This makes existing analytical approaches to calculate backwater rise at bridges unsuitable for extreme flood events, since they consider solely natural debris components. Lyn et al. (2003), Okamoto et al. (2021) and Panici and de Almeida (2020) concluded that the shape of wooden logs affects the probability of bridge blockage and the porosity of debris accumulations. Panici and de Almeida (2020) questioned the accuracy and applicability of experimental results derived solely from idealized log shapes. In addition, Bayón et al. (2024) classified large objects that can be transported during urban floods and concluded that these can have a higher clogging potential. Such large objects could increase the potential to damage buildings and other infrastructure, as previously shown for tsunamis and coastal storm surges (Stolle et al. 2017; Wüthrich et al. 2020). Chowdhury et al. (2024) demonstrated that mixed debris accumulations lead to increased backwater rise at racks and increased loads on buildings. As Tubaldi et al. (2022) pointed out, current bridge design guidelines often underestimate loads for submerged decks and high blockage ratios. Overall, this highlights the importance of debris accumulation for flood risk management in general and the need to improve physical modeling approaches for backwater effects in rivers (Friedrich et al. 2022), incorporating effects of mixed and anthropogenic debris.

The hydraulic conditions at bridges during flood events depend on the discharge and hydromorphological conditions in the river section as well as the bridge geometry. Schalko (2018) and Panici and Kripakaran (2021) included the Froude number of the approach flow Fr_0 in a design equation on backwater rise at debris racks, which delivers higher backwater rise with increasing Froude number. In comparison to debris racks, bridges can further alter flow conditions during flood events due to the presence of bridge piers, bridge deck, and handrails. So when water levels reach or exceed the bridge deck, such as during the 2021 floods in Belgium and Germany (Poppema et al. 2025), the design of the bridge railing, deck and opening shape start to play an essential role in both the flow resistance of the bridge itself as well as in the debris accumulation process.

Motivated by these large and heterogeneous debris accumulations observed in 2021, Burghardt et al. (2024b) conducted new flume experiments to investigate backwater rise in the presence of natural and anthropogenic floating debris. With the help of a multi-laboratory approach, allowing the parallelization of experiments, a large dataset of over 250 test results was created. The aim of this study is to determine the effect of debris composition, hydraulic conditions, and bridge design on backwater rise at clogged bridges. The (preliminary) test results presented by Burghardt et al. (2024b) are analyzed in detail and extended by additional data, providing a comprehensive framework with a predictive equation, which can be used in practice to predict backwater rise associated with debris-induced bridge clogging.

Methodology

Laboratories and Flumes

This study is based on an experimental approach. The experiments were conducted in the hydraulic laboratories of TU Delft (the Netherlands), RWTH Aachen University (Germany), and Université de Liège (Belgium) under similar conditions, using three flumes with a width of 1.2 m and one flume of 1 m width. These flume characteristics are described in detail in Table 1, with flume codes (B1, B2, G1 and N1) named after the country (Belgium, Germany, the Netherlands). Flumes G1 and N1, which originally had larger flume widths, were narrowed to 1.2 m in order to ensure the same model conditions in all three laboratories. This corresponded to a 1:16 scaling ratio for the bridge model in the 1.2 m wide flumes (flume B1, G1, and N1), and a 1:19 scale in the 1.0 m wide flume (flume B2). Water levels (h) were measured with ultrasonic distance sensors (UDS) with an accuracy of 1 mm in all laboratories (Fig. 1). The position of sensors slightly varied between the four flumes due to technical limitations but remains within the same range. The Froude number of the approach flow was defined as $Fr_0 = v_0/(gh_0)^{0.5}$, where h_0 is the initial flow height, v_0 the initial flow velocity and g the gravitational acceleration. The flow velocity was defined as $v_0 = Q/(Bh_0)$ with Q being the discharge and B the flume width. The initial water level was defined at the bridge deck and controlled via a weir located on the downstream end of the flume (Fig. 1).

The same type of debris was used in all laboratories and added into the flume following the same protocol (for details, see the "Test Procedure and Program" section). Drop-in devices were installed, allowing to add batches of fixed volumes of debris oriented perpendicular to the flow. Debris that passed the bridge were collected at a downstream mesh. To further investigate interlaboratory differences in the approach flow conditions, upstream flow velocities were measured once at the beginning of each hydraulic set-up using acoustic doppler velocimeters (ADV) at least 3 m upstream of the bridge at 15 points uniformly distributed across the flow area (see Appendix).

Bridge Models

In order to determine the effect of bridge design on backwater rise, several bridge models were tested in this study. The fundamental bridge characteristics were based on average dimensions of bridges that experienced extreme debris accumulations during the 2021 floods

This work is made available under the terms of the Creative Commons Attribution 4.0 International license.

Table 1. Flume characteristics in the three laboratories

Flume characteristics	Liège (B1)	Liège (B2)	Aachen (G1)	Delft (N1)
Flume width (m)	1.2	1	1.7, narrowed to 1.2	1.5, narrowed to 1.2
Model scale (1: λ)	1:16	1:19	1:16	1:16
Flume length (m)	7.2	10	32	40
Flume height (m)	1.2	0.5	1.7	0.8
Slope (degrees)	0	0	0	0
Bottom/Wall materials	Metal	Glass	Concrete/plastered masonry wall	Concrete
Location of the UDS (m)*	4, 2.5, 1.5, 0.25,−1	4, 3, 2, 1,−0.5	4.5, 3.5, 2.5, 1.5, 0.25,−1	6.5, 3.5, 1.5, 0.25,−1
Maximum discharge (m^3/s)	0.25	0.2	1.2	0.1
Flow equalization	Synthetic screen at inflow	Metal grid and synthetic screen at inflow	Cubic flow equalizer at inflow	Ramp with flow guides
Location of the downstream weir (m)*	−2.5	−2.5	−4	−27
Orientation of the downstream mesh	Horizontal	Horizontal	Horizontal	Vertical
Location of the drop-in device (m)*	3.5	5.5	5	5.5
Height of the drop-in device above flume bottom (m)	0.8	0.5	1.2	0.8
Position of cameras	Side and top view at bridge	Side view at bridge	Side and top view at bridge	Top view at bridge
Location of velocity measurements (m)*	3.5	5.5	4.5	4
Conditions for velocity measurements	$Fr_0 = 0.27$, $h_0 = 27$ cm	$Fr_0 = 0.25$, $h_0 = 21.1$ cm	$Fr_0 = 0.27$, $h_0 = 27$ cm	$Fr_0 = 0.15$, $h_0 = 27$ cm

Note: *Locations given in meters against the flow direction with regard to the zero set at the downstream edge of the bridge.

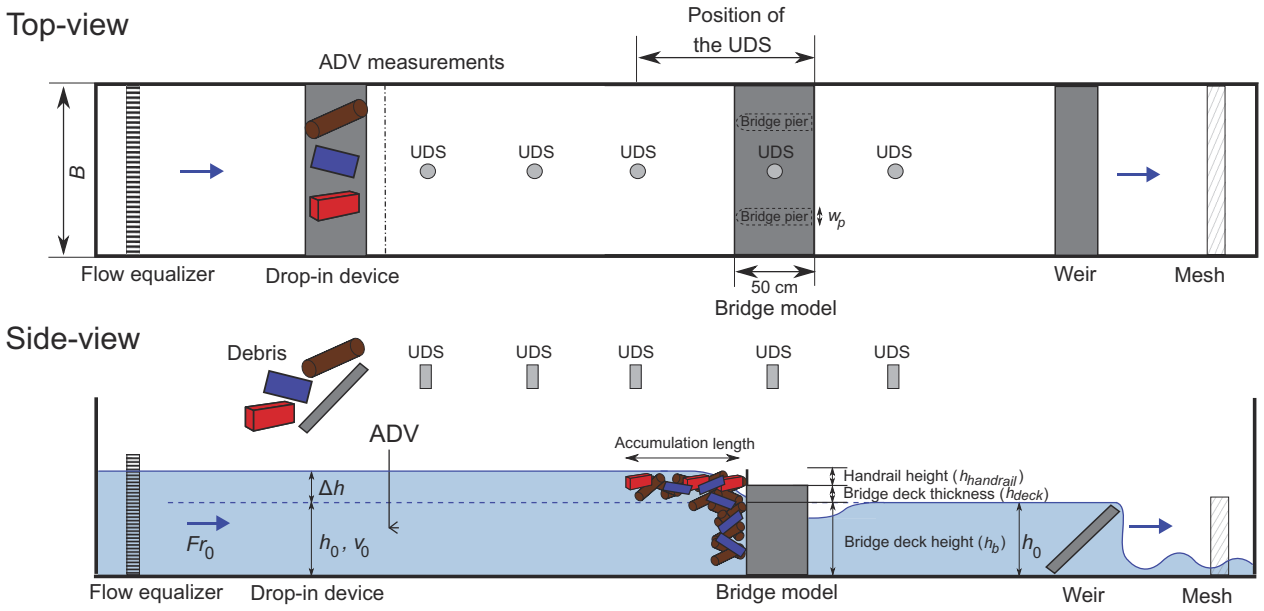


Fig. 1. (Color) Schematic overview of the set-up used in all three laboratories. Exact positions of drop-in device, UDS, weir and downstream mesh are provided in Table 1.

in Belgium and Germany, as reported by Erpicum et al. (2024) and Poppema et al. (2025). This resulted in a prototype bridge with two piers (n_p), each 1.1 m wide (w_p), and a central opening span of 8.5 m. The total width of the prototype bridge therefore amounts to 19.2 m with a depth of 8 m and an opening height of 4.3 m (h_b). The mean documented handrail height (h_{handrail}) was one meter, the thickness of the bridge deck 1.2 m (h_{deck}).

Several variations of this prototype bridge geometry were tested to assess the effect of bridge design, and the scaled bridge dimensions are displayed in Fig. 2. The effect of the number of bridge piers on the debris accumulation was investigated in flumes B2 and G1 by decreasing the number of piers to one centrally positioned pier or no bridge pier, where in flume B2 a slightly smaller bridge deck without handrail was used. The effect of bridge opening shape was studied by implementing an arched bridge in flume G1, since many arched bridges were damaged during the 2021 floods. Both bridges in flume B1 and G1 had the same number of piers (n_p), pier width (w_p) and deck thickness (h_{deck}, measured at the top of the arch), but the blockage ratio β_{bridge} ($A_{\text{frontal, bridge}}/Bh_b$) of the arched bridge was higher due to the circular deck shape. The frontal area of the bridge ($A_{\text{frontal, bridge}}$) is composed of the area covered by bridge deck, piers, and handrail. The frontal area of the handrail can be expressed with the help of the handrail porosity (Φ_{handrail}). Therefore, the frontal area of the bridge results to $A_{\text{frontal, bridge}} = A_{\text{frontal, deck}} + A_{\text{piers}} + A_{\text{handrail}} \cdot (1 - \Phi_{\text{handrail}}) = Bh_{\text{deck}} + n_p w_p h_b + Bh_{\text{handrail}} \cdot (1 - \Phi_{\text{handrail}})$. During the test

This work is made available under the terms of the Creative Commons Attribution 4.0 International license.

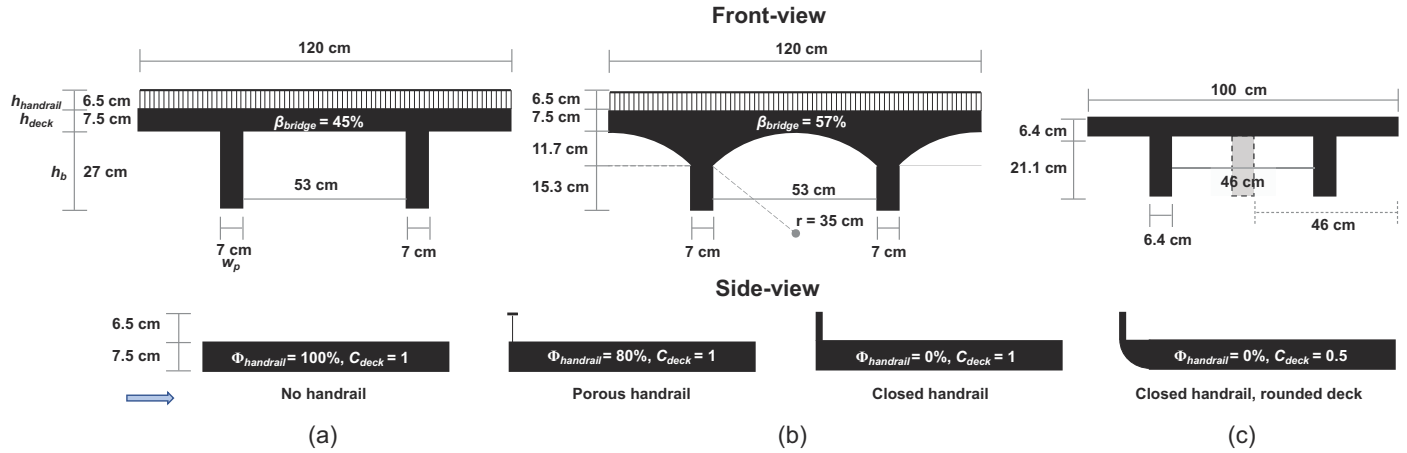


Fig. 2. (Color) Top row: Bridge models in front-view with (a) a rectangular; (b) arched opening shape for flumes B1, G1, and N1; and (c) the rectangular bridge for flume B2 with two pier configurations. All bridges measured 50 cm in the flow direction. Bottom row: Side view of all four handrail variations for model scale 1:16. The blue arrow indicates the flow direction.

Table 2. Debris compositions per batch for tests conducted for V_D = 76 L (12 batches per test)/190 L (test series 1, 30 batches per test). Configurations marked with "-" were not tested

Batch composition	No. of batches	Number of cubes	Number of plates	Number of logs per log length								d_{Dm} (m)	
				80 cm	70 cm	60 cm	50 cm	40 cm	30 cm	20 cm	10 cm	1:16	1:19
100% logs	40	0	0	¾[a]	1 ¼[a]	2	3	5	10	20	50	0.022	0.02
25% cubes, 75% logs	12/30	14/12[a]	0	¾[a]	1 ¼[a]	2	3	5	10	20	50	0.027	0.025
25% plates, 75% logs	12/30	0	127	¾[a]	1 ¼[a]	2	3	5	10	20	50	0.026	0.024
50% plates, 50% logs	40	0	190	⅜[a]	⅝[a]	1	1 ½[a]	2 ½[a]	5	10	25	0.033	—
50% cubes, 50% logs	20	3 ¼[a]	0	¾[a]	1 ¼[a]	2	3	5	10	20	50	0.037	—
20% plates, 20% cubes, 60% logs	24	1 ⅛[a]	127	¾[a]	1 ¼[a]	2	3	5	10	20	50	0.031	—
30% plates, 30% cubes, 40% logs	32	1 ¼[a]	143	⅜[a]	⅝[a]	1	1 ½[a]	2 ½[a]	5	10	25	0.032	—

[a]Fractions divided over batches, i.e., every sixth batch two cubes, every fourth batch no log of 80 cm length and two of 70 cm.

program, rectangular and arched bridge models were exchanged between flumes B1 and G1 and tested under the same flow and debris conditions to identify possible influences of the blockage ratio on backwater rise and interlaboratory differences.

Regarding handrail design, most bridge models had a porous handrail, composed of 2 mm thick steel bars and a guard rail on top, resulting in a porosity of approximately 80%. In flumes G1 and N1, the effect of different handrail porosities and bridge deck shapes (C_{deck}) on debris accumulation and backwater rise was investigated (Fig. 2, bottom row). Besides bridges with porous handrail, bridges with a solid handrail ($\Phi_{\text{handrail}} = 0\%$, $C_{\text{deck}} = 1$) or no handrail and flat bridge deck ($\Phi_{\text{handrail}} = 100\%$, $C_{\text{deck}} = 1$) were tested. Additionally, the impermeable handrail was combined with a rounded edge on the lower side of the deck ($C_{\text{deck}} = 0.5$) based on Schmocker and Hager (2011). In order to achieve higher Froude numbers in flume N1, the bridge deck was lowered from 27 to 20 cm at a certain point. A full overview of the test program is given in Tables 2 and 3.

Debris Compositions

The debris mixtures were based on the data collected by Erpicum et al. (2024) on visible debris accumulations during the 2021 flood event. It was observed that approximately half of the debris volume consisted of driftwood, and the other half of various man-made objects. Poppema et al. (2025) analyzed the shape of the debris in these accumulations, categorized them as percentages of logs, flat objects (e.g., building rubble, compressed caravans) and voluminous objects (e.g., vehicles, tanks, furniture). Based on this analysis, seven distinct debris compositions of logs, cubes, and plates were selected for investigation in the experiments (see Table 2).

Across all laboratories, the same debris at a 1:16 model scale was used to minimize interlaboratory differences (Fig. 3). Trees were mimicked by logs without roots or branches, with lengths between 10 and 80 cm, a 1/20 diameter/length ratio and with a length distribution based on Rickli et al. (2018) (see Table 2). Applying the weighted average log diameter $d_{Lm} = \sum(d_L^2 L_L)/\sum(d_L L_L)$ by Poppema and Wüthrich (2024), this results in a d_{Lm} of 0.022 m, where $1/d_{Lm}$ is representative for the frontal area per log volume. Log density varied between 400 to 600 kg/m^3 depending on the wood type used for each log length. Plywood plates ($10 \times 6 \times 0.2$ cm, painted blue) represented flat objects. Solid cubes of Douglas fir ($9 \times 9 \times 18$ cm, painted red) represented voluminous objects. To account for the size of these anthropogenic debris components, the formula for the weighted average log diameter d_{Lm} by Poppema and Wüthrich (2024) can be adapted, resulting in the weighted average debris diameter d_{Dm} [Eq. (2)]. Since $1/d_{Lm}$ represents the frontal area per debris volume, the surface area of the debris components facing the flow has to be determined, which is circular for logs and rectangular for plates and cubes. The difference in surface area shape is accounted for by the factor $4/\pi$ in Eq. (2). For this study, it is assumed that all debris components are predominantly oriented perpendicular to the flow based on the experimental procedure and observations during the

This work is made available under the terms of the Creative Commons Attribution 4.0 International license.

Table 3. Overview over the experiments conducted in all laboratories with two debris compositions for modeling series 2 and 3

	Bridge design			Hydraulic condition		Repetitions per debris composition (debris volume)	
Flume	Opening shape	Handrail design ($\Phi_{handrail}$, C_{deck})	n_p	Fr_0	h_0 (cm)	25% plates, 75% logs (V_D = 76 L or 50.7 L)	25% cubes, 75% logs (V_D = 76 L or 50.7 L)
B1, series 3	Rectangular	$\Phi_{handrail} = 80\%$, $C_{deck} = 1$	2	0.13	27	2	2
	Arched	$\Phi_{handrail} = 80\%$, $C_{deck} = 1$	2	0.27–0.28	27	2	2
					34	2	2
				0.4	30	1	2
B2	Rectangular	$\Phi_{handrail} = 100\%$, $C_{deck} = 1$	1	0.2	37.5	1	1
				0.27	10	2	3
					20–21	2	1
					24	2	2
					31	2	2
				0.4	10	2	3
					20–21	2	2
					24	2	2
				0.6	10	2	2
					20–21	2	2
B2	Rectangular	$\Phi_{handrail} = 100\%$, $C_{deck} = 1$	2	0.13	20–21	4	4
				0.2	37.5	1	1
				0.27	10	2	4
					15	2	2
					20–21	4	4
					24	2	2
					31	2	1
				0.4	10	2	2
					15	2	2
					20–21	2	2
					24	2	2
				0.6	10	2	2
					15	2	2
					20–21	2	2
G1	Arched	$\Phi_{handrail} = 80\%$, $C_{deck} = 1$	2	0.13	27	2	1
				0.28	15.3	2	2
					22	2	1
					30	2	2
					34	2	2
				0.4	15.3	2	2
					22	2	2
					27	2	2
					30	2	2
					34	2	2
				0.5	15.3	2	2
					22	2	2
					27	2	2
	Rectangular	$\Phi_{handrail} = 80\%$, $C_{deck} = 1$	2	0.28	22	—	1
					27	2	2
					39	2	—
				0.4	27	2	2
			0	0.28	27	—	1
					39	—	1
		$\Phi_{handrail} = 0\%$, $C_{deck} = 1$	2	0.28	34	—	1
					39	—	1
		$\Phi_{handrail} = 100\%$, $C_{deck} = 1$	2	0.28	34	2	—

This work is made available under the terms of the Creative Commons Attribution 4.0 International license.

Table 3. (*Continued.*)

Flume	Bridge design: Opening shape	Bridge design: Handrail design ($\Phi_{handrail}$, C_{deck})	n_p	Hydraulic condition: Fr_0	Hydraulic condition: h_0 (cm)	Repetitions per debris composition (debris volume): 25% plates, 75% logs (V_D = 76 *L* or 50.7 *L*)	Repetitions per debris composition (debris volume): 25% cubes, 75% logs (V_D = 76 *L* or 50.7 *L*)
N1	Rectangular (bridge deck at 27 cm)	$\Phi_{handrail}$ = 80%, C_{deck} = 1	2	0.13	22	3	1
					27	2	2
					33	1	2
				0.21	22	—	1
					24	2	—
	Rectangular (bridge deck at 20 cm)	$\Phi_{handrail}$ = 80%, C_{deck} = 1	2	0.15	27.5	3	—
					32	3	—
		$\Phi_{handrail}$ = 100%, C_{deck} = 1	2	0.15	27.5	3	—
					30	—	1
		$\Phi_{handrail}$ = 0%, C_{deck} = 1	2	0.15	27.5	4	—
					32	3	—
		$\Phi_{handrail}$ = 0%, C_{deck} = 0.5	2	0.15	27.5	6	—
					32	3	—

Note: $\Phi_{handrail}$ refers to the handrail porosity, C_{deck} to the bridge deck shape and n_p to the number of piers. Debris volumes V_D given for both model scales (1:16 or 1:19).



Fig. 3. (Color) Debris components with assumed orientation perpendicular to the flow direction: logs; plates; and cubes (not to scale).

experiments (see Figs. 3 and 4). This results in Eq. (2) and weighted average debris diameters as reported in Table 2, with a log diameter d_L, log length L_L, cube width w_C of 9 cm, cube length L_C of 18 cm, plate thickness w_{Pl} of 2 mm, plate height h_{Pl} of 6 cm, and plate length L_{Pl} of 10 cm

$$d_{Dm} = \frac{4}{\pi}\frac{\sum 0.25\pi d_L^2 L_L + \sum w_C^2 L_C + \sum w_{Pl} h_{Pl} L_{Pl}}{\sum d_L L_L + \sum w_C L_C + \sum h_{Pl} L_{Pl}} \quad (2)$$

During the tests, debris was dropped into the flume in batches, to measure the backwater rise as a function of debris volume. The initial tests in flume B1 and G1 focused on debris composition and critical amount of debris to capture main backwater rise, the total debris volume for each of the seven mixtures was 190 L divided into 20 to 40 equal batches (Table 2). During the second test series and to test the effect of hydraulic conditions on backwater rise, only the two debris compositions containing 75% of logs and 25% of plates or 25% of cubes were used, with 12 batches, i.e., 76 L per test. At model scale 1:19, the log distribution was adapted by omitting logs of 80 cm length, resulting in a d_{Dm} of 0.02 m, and the total debris volume was reduced to 50.7 L.

Test Procedure and Program

In total, 259 experiments were conducted to study the debris compositions and bridge designs as described in the previous sections. During the experiments, debris batches were added to the flume every 3 min from the drop-in device to ensure consistent debris orientation, perpendicular to the flow. Debris components that bypassed the bridge were collected at the downstream mesh and immediately readded upstream, to ensure that the accumulation volume at the bridge equals the total dropped-in debris volume at the end of each experiment. The debris accumulation length, defined as the horizontal distance between the bridge and the upstream edge of the accumulation, was measured 3 min after the last batch of debris was added (see also Fig. 1). The debris was dried overnight and shortly between the tests in each laboratory to ensure floating behavior. The test program was divided into the following series, focusing on three influencing factors for backwater rise, as detailed in Tables 2 and 3.

1. Effect of debris composition

   Initially, tests with a large debris volume $V_D = 190L$ and the seven debris compositions detailed in Table 2 were conducted in flumes B1 and G1. Results of these pre-tests in flume

This work is made available under the terms of the Creative Commons Attribution 4.0 International license.

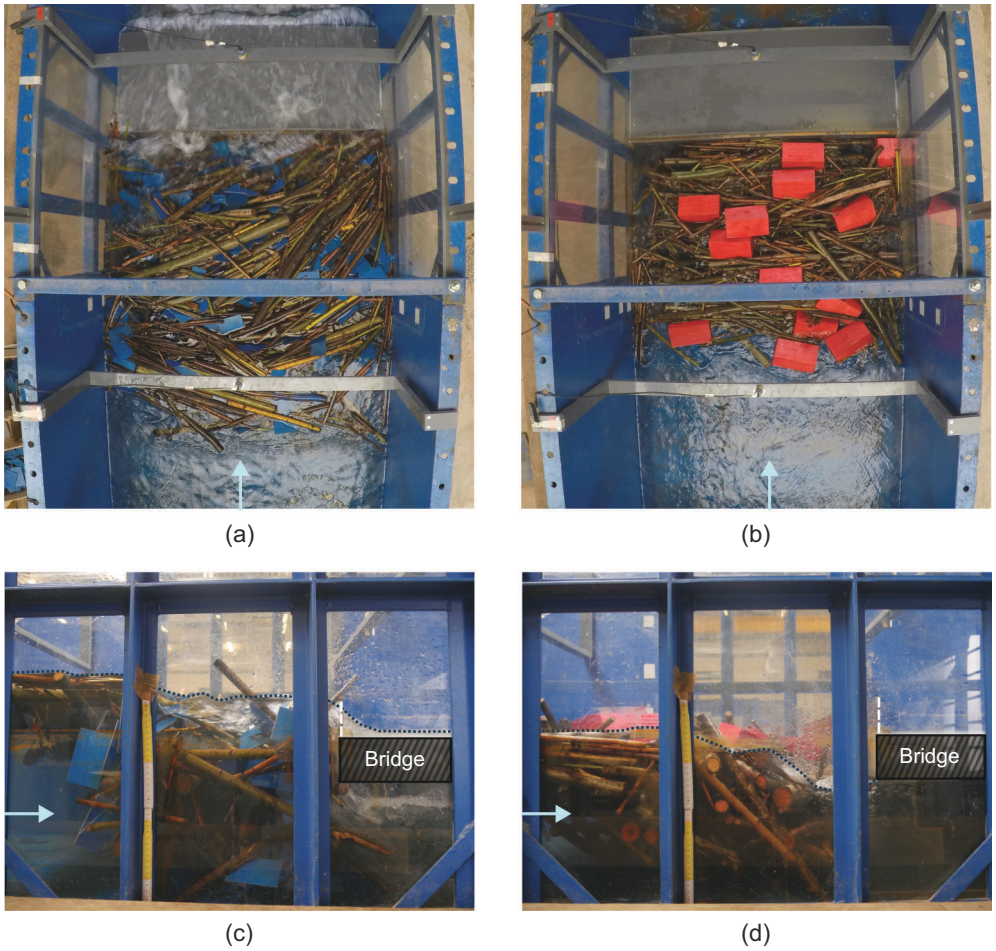


Fig. 4. (Color) The accumulation length and shape for two debris compositions in flume B1 with $h_0 = 27$ cm, $Fr_0 = 0.28$, $V_D = 76$ L. Top row: Top views with (a) 25% of plates and 75% of logs; and (b) 25% of cubes and 75% of logs. Bottom row: (c and d) side view of the same tests. Arrows indicate the flow direction, dotted lines the water level, dashed lines the handrail and dashed box the bridge deck.

B1 are called B1, series 1. These tests were conducted at fixed hydraulic conditions, with $Fr_0 = 0.27 - 0.28$, and the initial water level h_0 at the bottom of the bridge deck ($h_0 = 27$ cm).

2. Effect of hydraulic conditions

   In the second series, the effect of initial hydraulic conditions (i.e., Froude number and initial water level [h_0]) on backwater rise and debris accumulations was determined. This was investigated with a reduced debris volume of $V_D = 76L$ for $\lambda = 16$, based on the characteristic LW volume $V_c = 3.1Fr_0Bh_0^2$ as defined by Schalko (2018) for a fixed bed at $Fr_0 = 0.28$ and $h_0 = 27$ cm. For $\lambda = 19$ in flume B2, an equivalent volume of 50.7 L of debris was used.

3. Effect of bridge deck design

   Lastly, using the same debris mixtures, effects of the bridge design on backwater rise were examined by varying the opening shape, number of bridge piers and handrail designs in flumes G1, N1 and B1 (see section on bridge models). Tests results recorded in flume B1 during this experimental phase are referred to B1, series 3.

Dimensional Analysis

Model dimensions were determined using Froude similarity law, which was selected because all experiments involved open-channel flow under turbulent flow conditions ($Re > 10^4$) in which inertia and gravity are the dominant processes. This is in line with recent studies on LW transport and backwater rise at hydraulic structures (Panici and Kripakaran 2021; Piton et al. 2023; Schalko 2018; Wallerstein et al. 2001). Based on the test program, relative backwater rise $\Delta h/h_0$ is best described by the parameters listed in Table 4. The total debris volume V_D results from the sum of V_{cubes}, V_{plates}, and V_{logs}.

In total, 16 parameters were identified for the test program. With the three reference dimensions length, mass and time included in these parameters, according to the Buckingham Π-theorem, 13 nondimensional parameters $\Pi_{1\text{-}13}$ are obtained from the following dimensional analysis: Froude number $\Pi_1 = Fr_0 = v_0/(gh_0)^{0.5}$; relative log length $\Pi_2 = L_L/d_{Dm}$; percentage of cubes $\Pi_3 = V_{\text{cubes}}/(V_{\text{cubes}} + V_{\text{plates}} + V_{\text{logs}}) = V_{\text{cubes}}/V_D = \eta_{\text{cubes}}$; percentage of plates $\Pi_4 = V_{\text{plates}}/V_D = \eta_{\text{plates}}$; bridge blockage ratio $\Pi_5 = A_{\text{frontal, bridge}}/(Bh_b) = \beta_{\text{bridge}}$; bridge deck shape $\Pi_6 = C_{\text{deck}}$, relative water level $\Pi_7 = h_0/h_b$; the relative debris volume $\Pi_8 = V_D/(Bd_{Dm}h_0)$; relative bridge deck height $\Pi_9 = h_b/B$; relative velocity head $\Pi_{10} = ((v_0)^2)/(2gL_L)$; relative debris density $\Pi_{11} = \rho_D/\rho_W$; Weber number $\Pi_{12} = (\rho_W v_0^2 h_0)/\sigma$; and debris Reynolds number $\Pi_{13} = (v_0 d_{Dm})/\nu$.

Data on bridge and debris dimensions are based on field data of real flood events which facilitates the upscaling of the experimental results. The relative log length $\Pi_2 = L_L/d_{Dm}$, adopted from Rickli et al. (2018), was kept constant across all flumes in these experiments. The effect of the bridge deck shape $\Pi_6 = C_{\text{deck}}$ was solely assessed qualitatively, while debris density and fluid characteristics

J. Hydraul. Eng., 2026, 152(6): 04026038

This work is made available under the terms of the Creative Commons Attribution 4.0 International license.

Table 4. Parameters affecting the relative backwater rise, which can be found in the section on debris compositions (d_{Dm}, L_L, V_{cubes}, V_{plates}, V_{logs}, ρ_D), Fig. 1 (B, h_0, v_0) and Fig. 2 (β_{bridge}, C_{deck}, h_b, $\Phi_{handrail}$)

Parameter category	Parameter	Symbol	Unit
Debris	Mean debris diameter	d_{Dm}	(m)
	Log length	L_L	(m)
	Volume of cubes	V_{cubes}	(m^3)
	Volume of plates	V_{plates}	(m^3)
	Volume of logs	V_{logs}	(m^3)
	Density of debris	ρ_D	(kg/m^3)
Bridge design	Frontal area of the bridge	$A_{frontal,\ bridge}$	(m^2)
	Shape coefficient for the bridge deck	C_{deck}	—
	Bridge deck height	h_b	(m)
Experimental set-up	Flume width	B	(m)
	Approach flow velocity	v_0	(m/s)
	Initial water level	h_0	(m)
Physical parameters	Gravitational acceleration	g	(m/s^2)
Fluid properties	Water density	ρ_W	(kg/m^3)
	Water surface tension	σ	(kg/s^2)
	Water kinematic viscosity	ν	(m^2/s)

were not varied as part of the experimental design. The Weber number is not considered since surface tension effects are deemed negligible. The Reynolds number is sufficiently large to minimize scale effects, which will also be clarified by comparing tests at various scales. Therefore, Π_2 and $\Pi_{10\text{-}13}$ are not included in the following analysis. As a result, the relative backwater rise observed in this study can be described as follows:

$$\frac{\Delta h}{h_0} = f\left(Fr_0, \frac{V_D}{Bh_0 d_{Dm}}, \beta_{bridge}, \frac{h_0}{h_b}, \eta_{plates}, \eta_{cubes}\right) \tag{3}$$

Results

Accumulation Process and Length

Visual observations showed that the debris composition had a strong impact on the clogging process, accumulation geometry and backwater rise. In fact, debris compositions with increasing share of plates were more interlocked, resulting in more compact accumulations and steeper fronts in the vicinity of the bridge compared to debris compositions with a similar percentage of cubes [Figs. 4(a and c) versus Figs. 4(b and d)]. While plates were distributed homogenously among logs across the entire debris volume, cubes tended to float near the surface. Accumulations with plates led to a higher backwater rise and therefore overtopping of the bridge for the test with plates, as visible in the side view images of Figs. 4(c and d) (and analyzed quantitatively later). In general, overtopping was observed at lower debris volumes, when plates were present in the debris volume, confirming a higher influence of plates on backwater rise.

For $Fr_0 = 0.27$ and higher, debris accumulations reached down to the flume bottom across the entire bridge opening [Figs. 4(c and d)]. This resulted in accumulations of short length and high compactness. In the vicinity of the bridge deck, a lowering of the water level due to acceleration and seepage through the accumulation was observed, which is not detected by the upstream water level sensors. At a lower Fr_0 of 0.13, the debris accumulation process showed different features. Since the flow was not strong enough to pull debris down towards the flume bottom, a long, floating debris carpet formed and backwater rise remained very limited. At these low Froude numbers, backwater rise is the result of head losses due to a flow underneath a rough obstacle rather than flowing through a porous medium.

Before the experiments, the initial flow depth h_0 was set in the flume. During the experiments, once debris was added into the flume, backwater levels started to rise (Fig. 5). The increase was faster at the beginning of the experiments, with a maximum rate of 4.63 mm/L and an average of 2.12 mm/L, while it slowly stagnated during the last phase of the experiments to 0.3 mm/L on average. The characteristic volume V_c as defined by Schalko (2018) denotes the volume of LW, which generates the primary backwater rise and after which the formation of a floating debris carpet at the water surface starts with less influence on backwater rise. For the results displayed in Fig. 5, V_c equals 73 L. In line with findings by Schalko (2018), the debris carpet was short at the beginning of the experiment, with any added debris still contributing to further vertical development of the accumulation. Once the accumulation volume exceeded approximately 80 L, the accumulation length steadily increased upstream with any additional debris volume. At the end of the test, when around 190 L of debris were added, the debris carpet reached (in some cases) the most upstream water level sensor, which measured the top of the debris carpet instead of the water surface. This resulted in invalid test data which were not considered in the later analysis.

The development of the debris carpet was not observed as a linear process. While the accumulation length remained rather small at the beginning of the experiments, it increased after a certain tipping point, when less debris was pulled under water and a floating carpet formed. The accumulation length for the total debris volume $V_D = 76\ \ L$ ranged between 0.8 and 4.5 m in all three flumes at model scale 1:16. The debris carpet was typically shorter for debris mixtures with cubes compared to those with plates. Only at $Fr_0 = 0.27$ and 0.28, the accumulation length between the two mixtures was similar and only a single repetition of the mixtures with plates led to a slighty shorter accumlation than the cubes. Despite the scatter, the final accumulation length overall decreased with increasing Froude number for both debris compositions (see trend Fig. 6). In contrast to the effect of Froude number, there was no significant correlation between the initial water level and the accumulation length.

Although the clogging probability was not the objective of this study, changes in hydraulic conditions and bridge geometry affected clogging behavior and therefore backwater rise measurements. No debris accumulation was observed for initial water levels above the handrail elevation since all debris passed over the bridge deck. The number of bridge piers had a visible effect on the clogging probability, with one pier allowing more debris to pass the bridge compared to the two piers configuration. This influenced the blockage probability but also made it difficult to initiate clogging. As a result, multiple test restarts were required before a stable accumulation formed, with the initial debris batches remaining at the bridge rather than being flushed through the flume. In line with this, it was not possible to initiate persistent clogging for bridge configurations without piers, for which no debris-induced backwater rise was measured. Changing the porous handrail to a closed handrail and a rounded deck also decreased the initial clogging probability; however, an accumulation still developed at a later stage of the experiment.

This work is made available under the terms of the Creative Commons Attribution 4.0 International license.

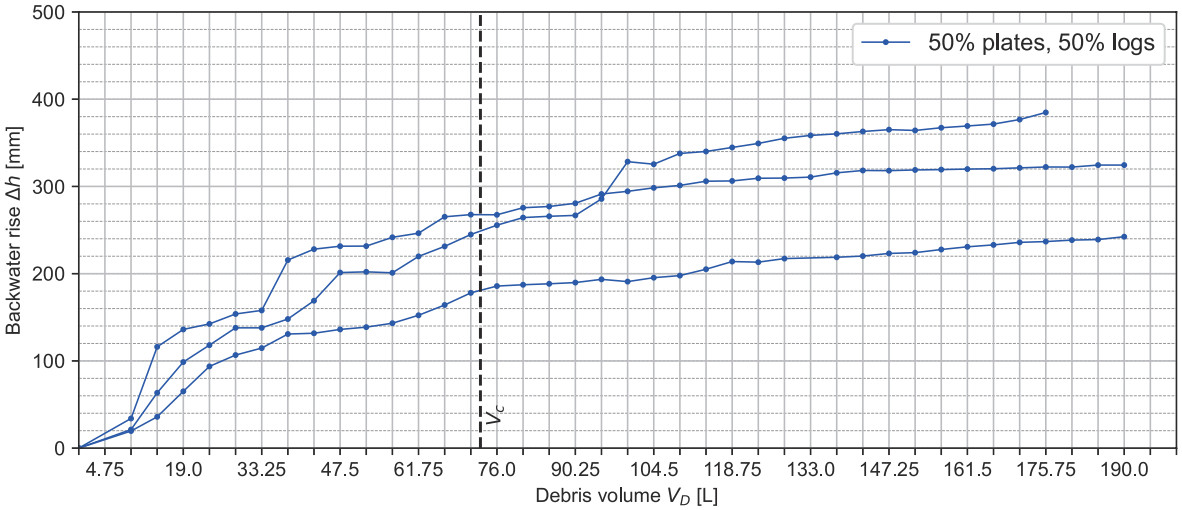


Fig. 5. (Color) Example of the development of backwater rise as a function of debris volume which was added in batches of 4.75 L. The tests are conducted in flume B1 with a debris composition of 50% plates and 50% logs. Backwater rise ($\Delta h = h - h_0$) was measured four meters upstream of the bridge. $Fr_0 = 0.27$; $h_0 = 27$ cm, with three test repetitions. Black dotted line indicates the critical volume V_c by Schalko (2018).

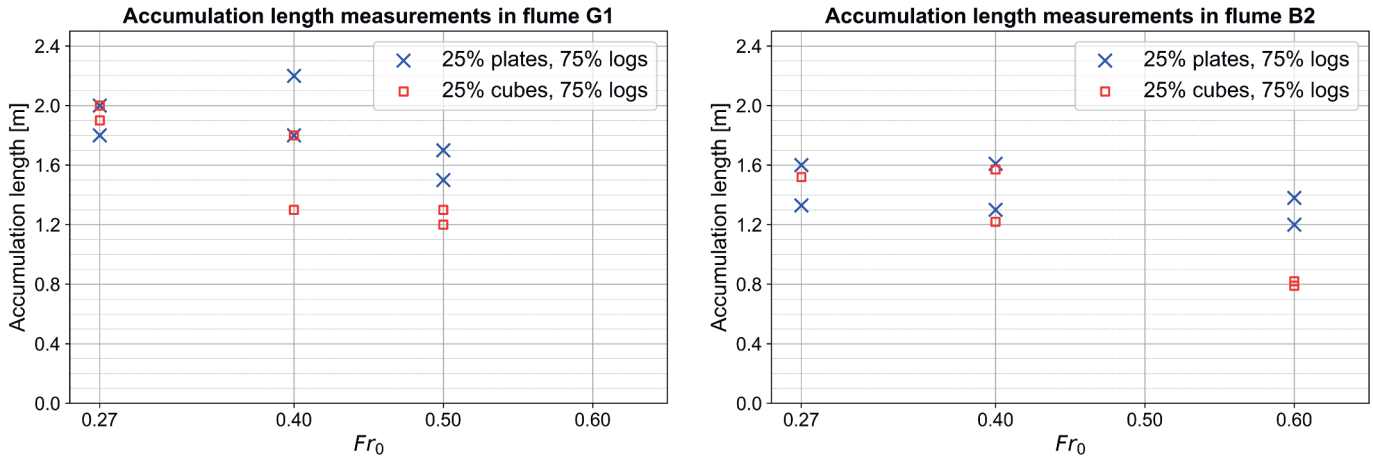


Fig. 6. (Color) Measurements of the accumulation length for two debris compositions in flumes G1 and B2 as a function of the initial Froude number at bridge models with rectangular opening shapes. The initial water level was just below the bridge deck at 27 cm in flume G1 and 20 cm in flume B2. The debris volume was 76 L in flume G1 and 50.7 L in flume B2.

Backwater Rise

This chapter evaluates the impact of the parameters outlined in the dimensional analysis on backwater rise. First, the effect of debris composition is examined, followed by an assessment of hydraulic conditions and finally, the influence of bridge design on backwater rise is explored. Based on these results, a predictive equation for estimating backwater rise at bridges was developed.

Backwater Rise: Effect of Debris Composition

The type and shape of debris components strongly influenced the magnitude of backwater rise upstream of a bridge. Fig. 7 shows the relative backwater rise $\Delta h/h_0$ after adding seven batches of various debris compositions ($V_D = 76$ L in total) in flume B1 and G1 for $Fr_0 = 0.27 - 0.28$ and $h_0 = 27$ cm, just below the deck. A relative backwater rise $\Delta h/h_0 = 1$ implies a doubling of the original upstream water level. Debris compositions containing plates and logs caused the highest increase, up to two times the original water level, which was 2.5 times higher than the relative backwater rise of debris composed only of logs. Lastly, regarding the variability, debris compositions containing plates showed a higher variation in final backwater rise with a range of 0.5 relative backwater rise around the mean and a relative standard deviation of up to 20% in flume B1.

In contrast, the lowest backwater rise was achieved for debris compositions with a high share of cubes. Mixed debris compositions, containing logs, cubes and plates also showed a strong backwater rise in flume B1 due to the presence of plates and reached up to 70% relative backwater rise on average, which is up to 1.7 times the relative backwater rise with only logs. However, this effect was not visible in flume G1. Applying the mean debris diameters stated in Table 2 and the accumulation type factor $f_A = 0.55$ to Schalko's equation [Eq. (1), Schalko 2018], results in the black crosses in Fig. 7. While these are applied for $Fr_0 = 0.27$ and 0.28, slightly below their validity range, test results in flume B1 for 100% of logs and 25% of cubes are in good agreement. For test results with 25% of plates and more diverse debris compositions, predicted backwater rise at debris racks by Schalko (2018) differs from the present study. Test results in flume G1 are not in agreement with Schalko (2018), likely due to the arched opening shape of the bridge, implying that debris composition as well as bridge design need to be more carefully considered to predict backwater rise.

This work is made available under the terms of the Creative Commons Attribution 4.0 International license.

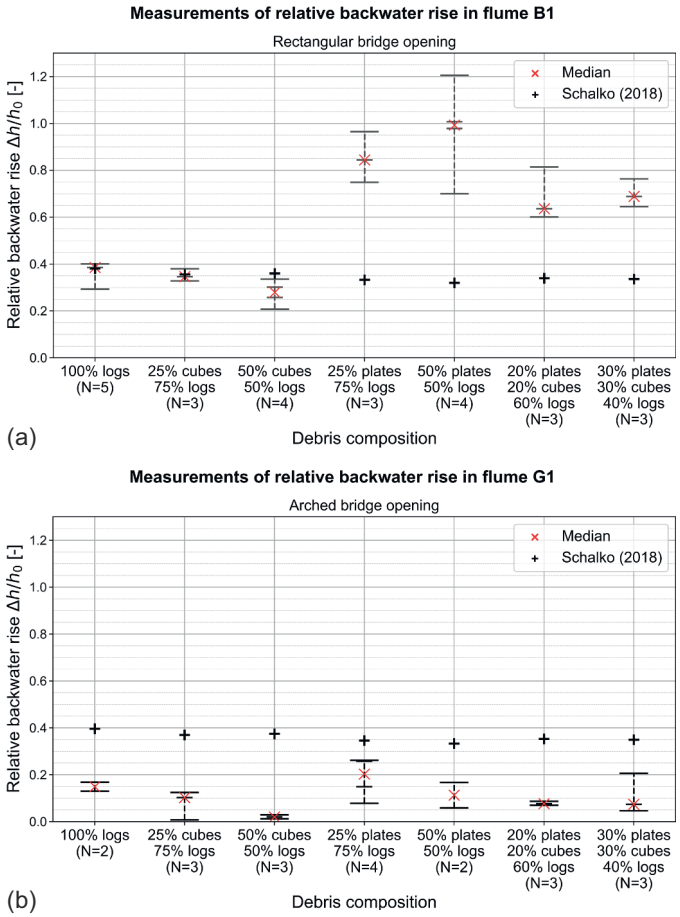


Fig. 7. (Color) Relative backwater rise for tests with different debris compositions during test series 1 in (a) flume B1 (rectangular bridge opening); and (b) flume G1 (arched bridge) for bridges with a porous handrail. Range indicates the interval between the minimum and maximum values, red cross the median value. Number of repetitions N is indicated in brackets. $Fr_0 = 0.27$ in flume B1 and $Fr_0 = 0.28$ in flume G1, $h_0 = 27$ cm, $V_D = 76$ L. "+" indicate results predicted by Schalko (2018) [Eq. (1)].

The range of backwater rise varied strongly between the flumes B1 and G1 during the first phase of the experiments (pretests, series 1). The initial test series in flume B1 led to more than twice as much relative backwater rise compared to the tests in flume G1 for all seven debris compositions. Although the bridge models differed in terms of opening shape between the two flumes, the significant backwater rise recorded in the initial series in flume B1 could not be reproduced under similar hydraulic conditions in subsequent tests in any other flume (see section on "Backwater Rise: Effect of Bridge Design"). Despite the difference in magnitude of backwater rise, the same effect of debris shape is clearly visible in both datasets, confirming that the presence of plates was associated with higher backwater rise. Variations between the two flumes could be minimized for the second and third test series with only 76 L of debris volume by changing the downstream mesh orientation from a vertical to a horizontal mesh in flume G1. Further, regular discharge controls and flow velocity measurements were introduced to ensure similar hydraulic conditions in all flumes.

Debris compositions with 25% of plates or 25% of cubes were considered to be the most realistic for the 2021 floods based on Poppema et al. (2025), providing reasonable upper and lower limits, respectively, for the extent of backwater rise of mixed compositions. Therefore, these two compositions were selected for the second and third series of modeling (Table 3).

Backwater Rise: Effect of Hydraulic Conditions

Results for flumes G1, B1 (series 3), B2 and N1 for debris compositions containing 75% logs and 25% cubes or 25% plates are compared in Fig. 8 for four initial water levels and increasing Froude numbers. Here, the final backwater rise at the end of the tests is compared, since its development over time was similar for all laboratories. These results highlight that tests conducted in different laboratories agree well, all showing increasing backwater rise for increasing Froude number. Test repetitions under the same conditions had relative backwater rise that varied on average by 4% for plates and 3% for cubes reaching a maximum of 13% standard deviation in flume B2. For comparison, tests conducted under the same hydraulic conditions and with higher Froude numbers did not reveal any higher variability. Current data are also compared with the design equation by Schalko (2018) for a natural accumulation with a fixed bed ($f_A = 0.55$), the weighted average debris diameters ($d_{Dm} = 0.026$ m for $\eta_{\text{cubes}} = 25\%$, $d_{Dm} = 0.025$ m for $\eta_{\text{plates}} = 25\%$) and a fine material content of 0% within the defined scope of $Fr_0 = 0.3 - 1.5$, shown in the black dotted lines in Fig. 8. While Schalko's equation for pure logjams slightly overestimates the backwater rise for the debris mixtures with 25% cubes, it underestimates the backwater rise for the mixtures with plates at Froude numbers above 0.4. This discrepancy slightly increases for higher relative initial water levels h_0/h_b, when water levels reach the bridge deck.

Since almost no backwater rise was observed for $Fr_0 = 0.13$, the threshold for absence of clogging induced backwater rise was set below Froude number 0.13, shaded in grey in Fig. 8. This is supported by findings of Follett et al. (2020) and Poppema and Wüthrich (2024), who concluded that for a given accumulation geometry the backwater rise increases more gently at low Froude numbers. Since only limited debris is pulled down to the channel bottom at low Froude numbers, backwater rise is almost absent, and the accumulation grows horizontally rather than vertically. Hence, head losses are mostly associated with enhanced shear stresses below the accumulation, similarly to what happens for plastic accumulations (Yan Toe et al. 2025). The measurements of carpet length in Fig. 6 further support this, since the carpet length decreases for higher Froude numbers, where the accumulation also grows vertically, forming a more compact accumulation.

Increasing the initial water level h_0 while keeping the same Fr_0, led to a slight increase in absolute backwater rise. However, a negative correlation between relative backwater rise $\Delta h/h_0$ and the relative initial water level h_0/h_b can be seen in Fig. 9, due to the more substantial increase in values for h_0. This trend applies also to higher Froude numbers, but not shown herein. Nevertheless, it was observed that the initial backwater rise was smaller for initial water levels around the top of the bridge deck. In this case, the first debris batches accumulated right in front of the bridge deck, where the bridge deck is already responsible to block the flow. These accumulations only start to generate substantial backwater rise once they grow large enough to block the open cross section by extending below or above the height of the bridge deck. Lastly, Fig. 9 confirms the effect of debris shape on backwater rise, with higher relative backwater rise associated with debris compositions with 25% of plates compared to 25% of cubes.

Backwater Rise: Effect of Bridge Design

Fig. 10 presents the results for two bridge opening shapes and their effect on relative backwater rise. Initially, test results in flume G1 with an arched bridge showed a lower relative backwater rise compared to the tests conducted in flume B2 with a rectangular bridge. The exchange of bridges between the two laboratories in the third test

This work is made available under the terms of the Creative Commons Attribution 4.0 International license.

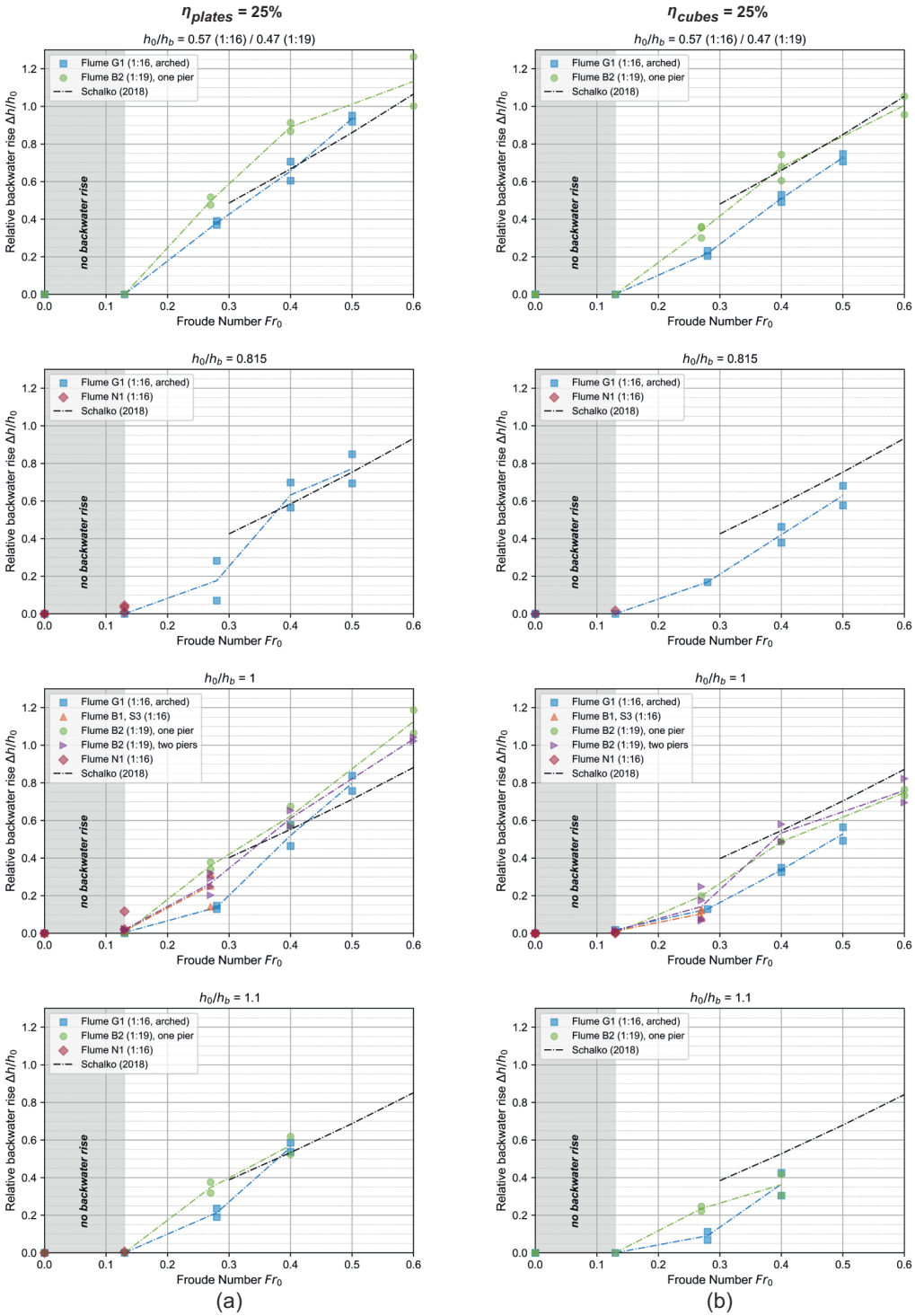


Fig. 8. (Color) Relative backwater rise for tests conducted in all three laboratories with both bridge designs and different relative initial water levels (h_0/h_b). Left column: Debris composition with 25% plates and 75% logs. Right column: Debris composition with 25% cubes and 75% logs. $V_D = 76 \quad L$ (scale 1:16) or 50.7 L (scale 1:19). Dotted lines connect averages for the various repetitions. The black line shows results of the design equation provided by Schalko (2018) for a natural accumulation at a fixed bed with 0% fine materials.

series of flume B1, led to more similar results between both flumes G1 and B1, with differences in backwater rise between flumes generally smaller than 6%. Here, it is also visible that backwater rise was lower for an arched opening shape with the same debris volumes, discharge and initial water level. This effect was most prominent for tests conducted with plates, where the relative backwater rise $\Delta h/h_0$ reduced on average from 0.29 to 0.17. For debris containing cubes, both opening shapes lead to nearly the same backwater rise. Results also indicate that the number of piers did not significantly affect the backwater rise associated with the debris, as shown in Fig. 8.

As discussed in the section on accumulation process and length, the initialization of clogging is less likely at closed (impervious) and rounded handrail designs. However, once clogging occurred, the backwater rise at the end of the test was higher at impervious handrails than at porous handrails (Fig. 11). Conversely, at bridges with no handrail, backwater rise due to debris was on average lower

J. Hydraul. Eng., 2026, 152(6): 04026038

This work is made available under the terms of the Creative Commons Attribution 4.0 International license.

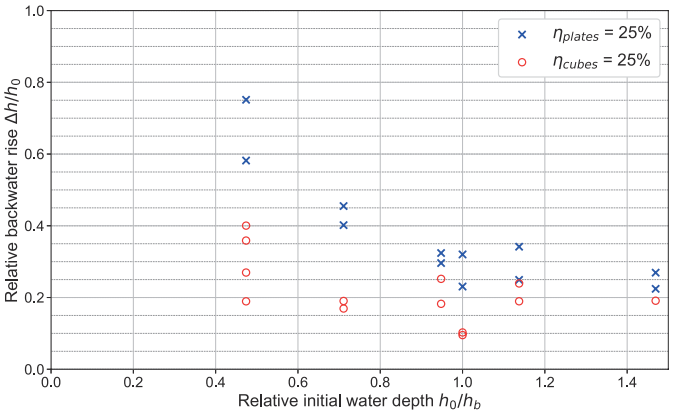


Fig. 9. (Color) Relative backwater rise ($\Delta h/h_0$) with regard to the relative initial water level in front of the bridge (h_0/h_b) for tests conducted in Flume B2 with two bridge piers, a rectangular bridge opening and at $Fr_0 = 0.27$.

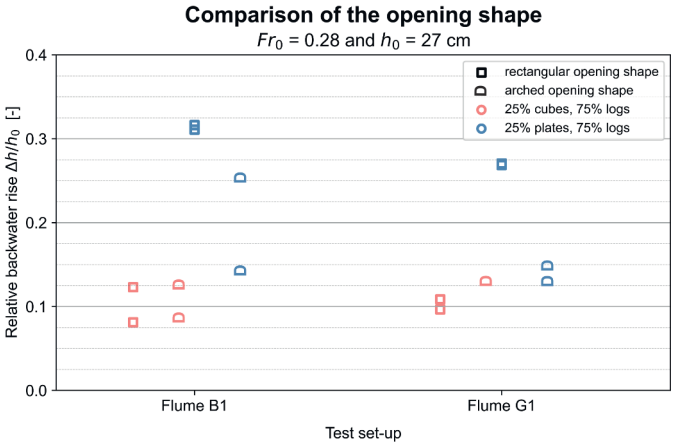


Fig. 10. (Color) Relative backwater rise of the exchanged bridge models in flumes G1 and B1 as a function of opening shape and debris composition. Tests were conducted with the initial water depth at the lower edge of the bridge deck ($h_0 = 27$ cm), $Fr_0 = 0.28$, 1:16 model scale, and $V_D = 76$ L. Rectangular opening shape refers to a β_{bridge} of 45%, arched opening shape to a β_{bridge} of 57%. Red symbols for debris compositions with 25% of cubes and 75% of logs, blue symbols for 25% plates and 75% logs.

than at porous handrails. Bridge opening shape and bridge handrail have an effect on the backwater rise due to the bridge structure itself, with higher blockage ratio and lower handrail porosity leading to a higher backwater curve.

Backwater Rise: Predictive Equation for Backwater Rise at Bridges

Results in the previous sections show the need for new predictive equations to quantify backwater rise for civil engineering design purposes. Applying the design equation that Schalko (2018) developed for backwater rise from uniform logs at debris racks [Eq. (1)], results in a disagreement with our experiments, with $R^2 = 0.67$, using the weighted average debris diameter d_{Dm}, $FM = 0$ and $f_A = 0.55$. In the dimensional analysis for the new predictive equation, the parameters Fr_0, $V_D/(Bh_0d_{Dm})$, β_{bridge}, h_0/h_b, η_{cubes}, and η_{plates} were identified as governing parameters for debris-induced backwater rise at bridges. With the help of a non-linear regression analysis, the design equation of Schalko (2018) was then extended by considering the bridge blockage ratio β_{bridge}, the relative water depth h_0/h_b, and the debris fractions η_{cubes}, η_{plates}. Specifically, Eq. (4) was calibrated using five parameters $\alpha_{1\text{-}5}$, based on final backwater rise of 183 tests conducted with seven debris compositions (as reported in Table 2), for $Fr_0 > 0.20$ and $0.47 < h_0/h_b < 1.78$ at bridges with porous or no handrails

$$\frac{\Delta h}{h_0} = \alpha_1 \cdot 5.4 \cdot 0.55 \cdot (\beta_{bridge})^{(\alpha_2)} \cdot \frac{h_0}{h_b}^{\alpha_3} \cdot \frac{Fr_0\left(\frac{V_D}{Bd_{Dm}h_0}\right)^{\frac{1}{3}}(1 + \alpha_4\eta_{plates} - \alpha_5\eta_{cubes})}{a} \tag{4}$$

The results of the multilinear regression can be summarized in the following equation:

$$\frac{\Delta h}{h_0} = 0.57 \cdot 5.4 \cdot 0.55 \cdot (\beta_{bridge})^{(-0.5)} \cdot \frac{h_0}{h_b}^{-0.17} \cdot \frac{Fr_0\left(\frac{V_D}{Bd_{Dm}h_0}\right)^{\frac{1}{3}}(1 + 0.5\eta_{plates} - 0.4\eta_{cubes})}{a}$$

$$\rightarrow \frac{\Delta h}{h_0} = 1.69 \quad f_A \quad \frac{1}{\sqrt{\beta_{bridge}}}\frac{h_0}{h_b}^{-0.17} \quad \frac{Fr_0\left(\frac{V_D}{Bd_{Dm}h_0}\right)^{\frac{1}{3}}(1 + 0.5\eta_{plates} - 0.4\eta_{cubes})}{a} \tag{5}$$

This equation results in a root mean square error of 0.12 and an R^2 of 0.83, confirming good agreement with the current data set, as shown by the comparison of experimental data and predicted values in Fig. 12. For low backwater rise (below 20%) at the lowest Froude numbers, the equation shows the poorest prediction accuracy. In this range, measurement uncertainties disproportionally affect the results, where only small backwater rise was recorded. The accuracy improves progressively with increasing Froude numbers. Still, the equation offers an extension of backwater rise predicted by Schalko (2018) at lower Froude numbers and is applicable for flood events with $0.2 < Fr_0 < 0.6$. For Froude numbers below 0.2, relative backwater rise was much lower and less than 12%, as debris was barely dragged down into the water column and instead formed a floating carped that induced little flow resistance. Applying $\beta_{bridge} = 35\%$, $\eta_{cubes} = 0\%$, $\eta_{plates} = 0\%$ at $h_0/h_b = 1$ to Eq. (5), determines the backwater rise solely at two bridge piers of a rectangular bridge opening for debris accumulations composed completely of logs and results in the same equation by Schalko (2018) for backwater rise at debris racks with a fixed bed and no fine material content (FM). Similar to Schalko's FM, plate-shaped debris components lead to an increase of backwater rise compared to accumulations composed solely of logs, whereas cuboid elements decrease backwater rise at bridges. Mathematically, this effect is expressed directly through the shape fractions (α_4, α_5) and indirectly through the weighted average debris diameter d_{Dm}. The larger the blockage ratio of the bridge, the smaller the debris

This work is made available under the terms of the Creative Commons Attribution 4.0 International license.

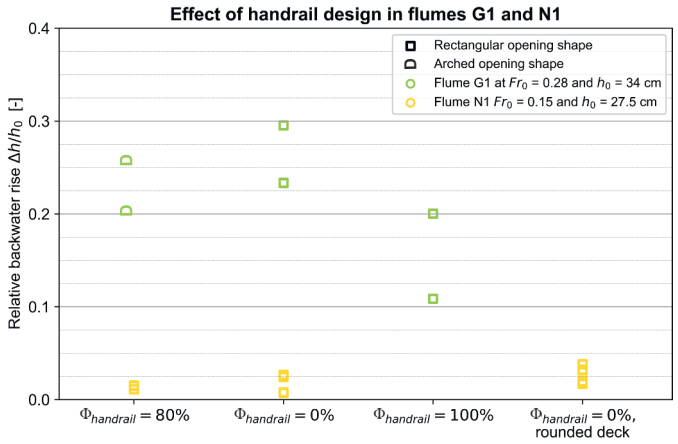


Fig. 11. (Color) Relative backwater rise as a function of handrail designs. Tests in flume G1 are conducted at $Fr_0 = 0.28$ with $h_0 = 34$ cm (at the top of the bridge deck) and in flume N1 at $Fr_0 = 0.15$ with a lowered bridge deck at 20 cm and $h_0 = 27.5$ cm (at the top of the bridge deck). Debris composition with 25% plates and 75% logs.

induced backwater rise at the bridge, since only debris, which accumulates at the bridge opening leads to additional backwater rise. The applicability of Eq. (5) is limited to bridge blockage ratios greater than zero, since debris blockage requires the presence of an obstacle that reduces the effective flow cross section. Lastly, relative backwater rise decreases with increasing relative initial water level (h_0/h_b), in line with the experiments.

Discussion

Experimental Results

This study investigated the effect of hydraulic conditions as well as debris composition and bridge design on backwater rise due to debris accumulations at bridges. In line with findings by Schalko (2018), Panici and Kripakaran (2021), and Schmocker and Hager (2013) for backwater rise at LW retention racks, the Froude number of the upstream approach flow was identified as a major factor influencing backwater rise at clogged bridges. Despite small variances in the magnitude of relative backwater rise, an increase in backwater rise was consistently observed for higher Froude numbers in all three laboratories. Accordingly, a lower debris volume was needed at higher Froude numbers to create the same backwater rise. The behavior of debris at the bridge was in line with findings by Okamoto et al. (2020), whereas the accumulation length increased for lower Froude numbers and trapped logs started to move downwards towards the channel bottom with increasing clogging of the bridge opening.

The debris composition was identified as a second major factor influencing backwater rise. Despite different magnitudes between flumes B1 and G1 during the pretests (series 1), backwater rise was substantially higher for debris compositions containing plates, while mixtures containing cubes led to lower backwater rise. This is conceptually in line with the design equation by Schalko (2018), since a higher share of fine material leads to a higher backwater rise compared to debris accumulations composed solely of logs. Similar to fine organic materials, plates can increase the flow resistance and reduce flow through the accumulation due to their large surface area when orientated perpendicular to the flow. Contrarily, cubes have a smaller surface area per debris volume and therefore caused less backwater rise. Still, cubes can have a large damage potential depending on their dimensions and density. These results, as well as

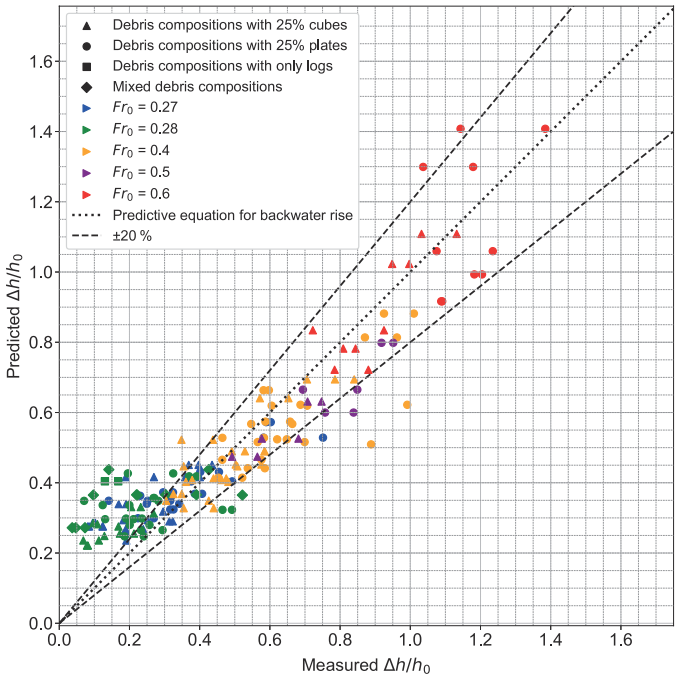


Fig. 12. (Color) Measured versus predicted relative backwater rise based on Eq. (5) with $\alpha_1 = 0.57$, $\alpha_2 = -0.5$, $\alpha_3 = -0.17$, $\alpha_4 = 0.5$, $\alpha_5 = 0.4$. Mixed debris compositions were used in test series 1 and contain plates, cubes, and logs.

the comparison to the design equation of Schalko (2018), show that man-made objects like plates can lead to higher backwater rise and larger flood damage than predicted by current estimations.

The opening shape, which determines the bridge blockage ratio, had a strong effect on the upstream flow conditions through their flow resistance which generated a backwater effect from the bridge itself, without debris (Majtan et al. 2024; Soori and Karami 2024). Similarly, the handrail design showed a clear effect on backwater rise. Bridges with closed handrails generated more backwater rise at initial water levels above the bridge deck height, even without debris, due to their higher blockage ratios, and produced an additional backwater increase once debris accumulated. This is likely because the higher blockage ratio induces greater flow velocities and Froude numbers beneath the bridge, which in turn amplify the backwater rise when debris in induced. Although clogging probability was not the main focus of this study, experiments showed that a rounded deck shape, lower number of piers or nonpermeable handrail all decreased the probability of debris being blocked at bridges, similar to the results of Schmocker and Hager (2011) and Bénet et al. (2021).

The application of a multiflume analysis facilitated the parallelization of test procedures and therefore the creation of a large dataset but also introduced uncertainties to the experimental results. Measurement errors were minimized by a regular calibration of water level sensors in all laboratories. Uncertainties in approach flow conditions might result from varying discharge, flume roughness and weir positions. Therefore, same approach flow conditions were applied to all flumes regarding Fr_0 and h_0 and checked with the help of velocity measurements, which showed only minor variances (see Appendix). While tests conducted in flumes N1, B2, and G1 yielded comparable results and led to similar conclusions, the first test series in flume B1 showed a pronounced discrepancy relative to the other tests results. In particular, compared with the tests in flume G1, the B1 series 1 tests produced nearly four times higher relative backwater rise. A possible factor for uncertainties

This work is made available under the terms of the Creative Commons Attribution 4.0 International license.

in these results could be the debris transport. Despite identical debris material, debris size and batch volumes across laboratories, unnoticed differences in debris transport could result from different debris densities, e.g., due to shorter drying phases in-between tests or the initial water content of the freshly cut wood. While Schalko (2018) assumed that the density of LW would not affect the clogging probability, Ruiz-Villanueva et al. (2014), Hartlieb (2015), and Panici and de Almeida (2018) indicated that debris density has a strong effect on the transport process of LW and can effect backwater rise. Differences in debris density might therefore have influenced the drag forces acting on the transported materials. Accordingly, a larger number of repetitions is recommended, along with continuous comparison of test results and the overall experimental procedure (e.g., using videos) to identify early occurrence of inter-laboratory differences, reduce uncertainties, and ensure the collection of reliable data.

Especially LW, which behaves randomly, requires a certain number of test repetitions to obtain statistically reliable results (Furlan et al. 2019; Schmocker and Hager 2013; Welber et al. 2013). Tullis et al. (2019) demonstrated that even simple experiments on the head-discharge relationship of a weir, conducted in different laboratories, can show differences up to 50%, originating from numerous sources such as differences in instrumentation type, calibration, approach flow conditions and human errors. Hence, this multilaboratory approach highlights the importance of conscientious uncertainty estimations for the parallelization of experiments and demonstrates the uncertainty range for debris accumulation processes. Even under controlled laboratory conditions, the accumulation processes showed considerable randomness, which may be even higher for natural accumulation processes. Single-laboratory experiments or test series with less repetitions might not be able to quantify these variations and might under- or overestimate test results. The predictive backwater rise equation derived herein [Eq. (5)] shows an overall good fit with the large number of test results. Small relative backwater rise below 20% is currently slightly overestimated which might be improved by additional tests. Finally, Eq. (5) highlights additional important factors, i.e., the shape of debris components and bridge design, which affect backwater rise at bridges during floods.

Limitations

The experiments conducted in this study are part of a systematic investigation of the effect of debris accumulation at bridges on the backwater rise during flood events. To conduct this systematic investigation, a number of simplifications were made, which led to a reduction in the complexity of the real system. These model and scale effects include a number of relevant aspects, discussed hereafter. First, the material properties of the elements (bridge, handrail, debris) were not scaled along with their size. Hence, the stability of bridge deck, handrail, and debris was much higher compared to reference bridges and natural wood. As a consequence, no bridge failure occurred, and no breaking of debris was observed, which might have happened in a natural flood event (Burghardt et al. 2024a). Notably, breaking of debris components might create different log distributions, which can change the accumulation properties (Piton et al. 2023; Schmocker and Hager 2011). Second, the logs, representing natural wood within the debris composition, were composed of natural branches in cylindric shape, which may differ in wood type and density from natural wood in a river. The shape of debris influences the stability of the debris accumulation, and log shapes with roots or branches might lead to less stable accumulations (de Cicco et al. 2020; Panici and de Almeida 2020). Lastly, changes in buoyancy due to prolonged soaking of the debris were not analyzed in detail. For anthropogenic debris components, averaged data by Erpicum et al. (2024) and idealized debris compositions by Poppema et al. (2025) were used to determine uniform plate and cube dimensions, while in reality elements with various dimensions were documented, potentially affecting backwater rise at bridges. These simplifications were necessary to perform systematic investigations under controllable and defined boundary conditions in the hydraulic laboratories. The effects of the aspects not considered in this study can be examined separately, and their findings can later be integrated with the existing results.

Apart from these model and scale effects stemming from the need of simplification, there are some limitations regarding the applicability of the predictive equation for backwater rise [Eq. (5)] developed in this study. These refer to the setup of the bridge and the interdependency with other flood-related processes in rivers. Within the test program, mostly homogenous flow fields were pursued and river slope, bed load transport, and dynamic water levels were neglected, which may differ from natural flood events. Further, the flows applied in this study were subcritical, which might amplify backwater rise. Natural flood processes are further influenced by the river bed conditions, scour, and sediment transport (Panici and Kripakaran 2021; Schalko 2018). By conducting the experiments in a fixed flume, river bed erosion and interactions with surroundings or the channel bottom were neglected, which may have a strong effect on clogging probability (Bezzola et al. 2002) and the extent of backwater rise (Schalko 2018). The conducted flume experiments resemble bridges in confined river sections within urbanized areas or in steep and narrow valleys, where bypassing of the bridge is not possible. Therefore, the developed equation is best applicable for these scenarios, including flood conditions where water levels rise between the midheight of the bridge opening and the top of the bridge handrail. As the equation has not yet been validated for other bridge configurations and hydraulic conditions, it may overpredict backwater rise in those scenarios. Lastly, since experimental data are based on flood, bridge, and debris characteristics from the 2021 flood event in Western Europe, the applicability of the backwater rise equation is best suited for extreme flood events, reaching large debris volumes and comparable debris compositions, as tested in this study. With the help of additional tests on further bridge and river dimensions, different scales and further debris densities, the applicability of the equation can further be extended.

Recommendations for Future Bridge Design and Operational Flood Protection

Based on these results, recommendations regarding bridge design, operational flood protection, and river maintenance can be drawn. Decreasing the probability of clogging and debris accumulation by reducing the number of piers, increasing the freeboard/bridge height and the span width of the bridge are recommended, in line with recommendations by Bénet et al. (2021), Schmocker and Hager (2011), and Bezzola et al. (2002). Once debris is blocked, results further show that the handrail can affect how much backwater rise is generated, with impermeable handrails generating more backwater rise. While debris at a permeable handrail was found to generate less backwater rise, permeable handrails increase blockage probability according to Schmocker and Hager (2011) due to debris entangling in the handrails. Hence, foldable or removable handrails could be a suitable alternative, which can be dismantled prior to the flood event or collapse as soon as certain hydrodynamic pressure occurs, allowing the transport of debris over the superstructure of the bridge at high water levels. For nonessential structures,

This work is made available under the terms of the Creative Commons Attribution 4.0 International license.

This work is made available under the terms of the Creative Commons Attribution 4.0 International license.

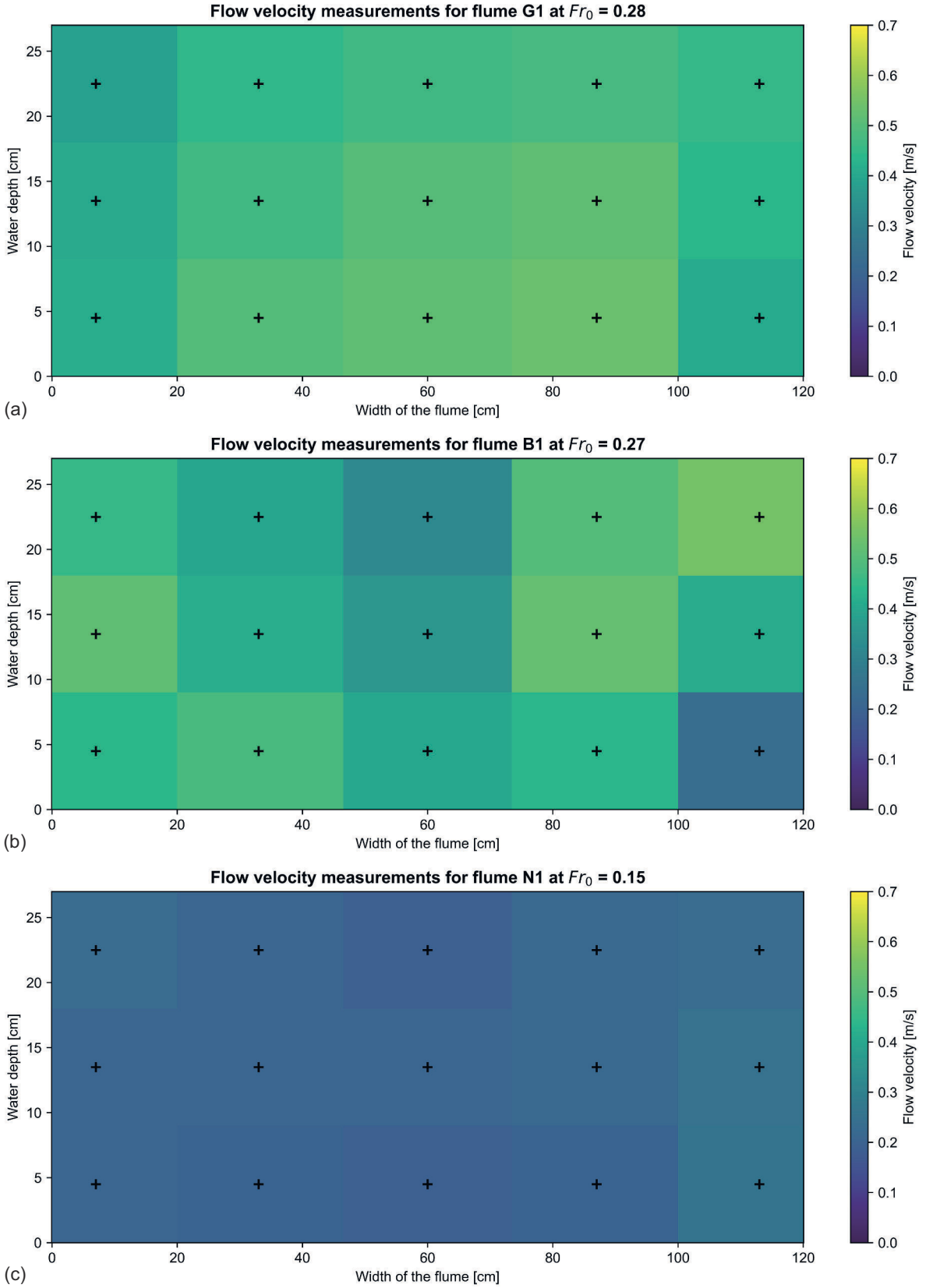


Fig. 13. (Color) Flow velocity measurements for (a) flume G1 in Aachen at $Fr_0 = 0.28$; (b) flume B1 series 3 in Liège at $F_0 = 0.27$; and (c) flume N1 in Delft at $Fr_0 = 0.13$, all with $h_0 = 27$ cm. Each measurement location is marked with a '+'.

such as hiking or cycling trails, installing (very) low bridges that intentionally flood during minor discharges (i.e., allowing most debris to pass over the deck) offers another viable option. In addition, this could facilitate guiding of debris toward dedicated retention measures, which are best located outside of densely populated areas (Panici and Kripakaran 2021; Schmocker and Hager 2013). Regarding the structural design of bridges, it is important to consider additional hydraulic loads due to backwater

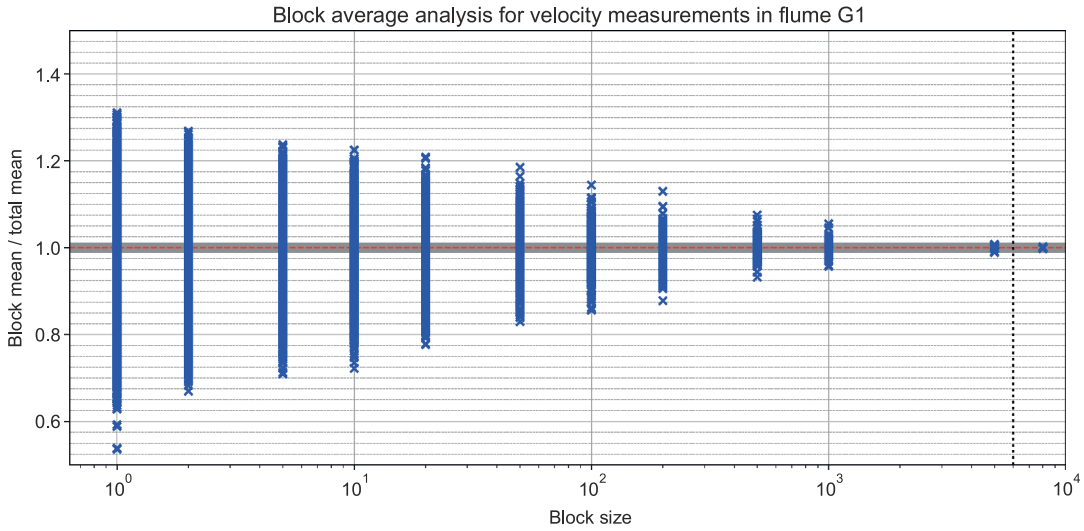


Fig. 14. (Color) Block average analysis for all flow velocity measurements at different positions conducted in flume G1 at $Fr_0 = 0.28$ and $h_0 = 27$ cm. The red dashed line indicates the total normalized mean (=1), and the gray shaded area marks a ±1% deviation around the total normalized mean. The vertical line corresponds to the 60 s measurement period, and the x-axis is plotted on a logarithmic scale.

This work is made available under the terms of the Creative Commons Attribution 4.0 International license.

rise (Parola et al. 2000), debris accumulation, and increasing flow velocities under or around the accumulation in order to prevent bridge collapse. As Tubaldi et al. (2022) noted, the hydraulic effects of bridges during flood events are often underestimated. Given our observations that anthropogenic debris can create denser accumulations and greater backwater rise, this underestimation is particularly critical in urban areas, where floods pose higher risks and are more likely to generate such debris. For these areas, this study further emphasizes the importance of accounting for debris accumulations at hydraulic structures in flood risk modeling and hazard mapping.

Conclusions and Outlook

Many recent floods, including the 2021 events, highlighted the relevance of debris accumulations at bridges due to their severe consequences and additional damage to surrounding areas. This study experimentally investigated the effects of debris accumulations at bridges focusing on hydraulic conditions, effect of bridge design and the shape of debris elements, which were shown to be highly heterogenous during recent flood events. With the help of physical models of complete bridges (including bridge deck and railing) conducted at three laboratories in Belgium, Germany, and the Netherlands, major influencing factors on backwater rise were determined and analyzed.

In line with former studies, the Froude number and the debris volume accumulating upstream of a bridge were identified as critical parameters. Backwater rise was found to be negligible for Froude numbers below 0.13. At higher Froude numbers, backwater rise was up to three times larger for accumulations containing plates (i.e., representing smaller 2D objects) compared to accumulations with just logs. This shows that current estimations for inundation depths and flood risk at bridges in urbanized environments might substantially underestimate risks. The effect of debris accumulations on flow conditions was already visible at low initial water levels, i.e., at the beginning of a flood, highlighting that inundation area, inundation depth and flow velocity are quickly affected, endangering the bridge's structural stability. Despite smaller variations between the three laboratories on the magnitude of backwater rise, similar processes and correlations were observed. With the help of this multilaboratory approach, a large data set of over 250 experimental results was created, introducing a new predictive equation to compute backwater rise as a function of debris composition, bridge design and hydraulic conditions within $0.2 < Fr_0 < 0.6$. To improve the applicability of this equation, further tests investigating the effect of model scale, debris density, and debris transport should be conducted in the future, expanding its validity to a broader range of configurations. These methodological considerations highlight the importance of physical models and result comparison under similar conditions during the development of a uniform methodology.

Overall, this study demonstrated the importance of understanding physical processes behind debris accumulations at hydraulic structures and the urgent need to consider these often-neglected phenomena in flood risk mapping. Despite large uncertainties regarding type, density, volume, and arrival times of floating debris, these findings offer valuable insights for practical engineers to assess and predict the consequence of worst-case clogging of critical infrastructures, contributing toward the development of more reliable flood protection strategies.

Appendix. Velocity Measurements

For all flume setups, the approach flow velocities were measured before the drop-in of debris at 15 points across the flow area (see Fig. 13). Velocity measurements were carried out for the flow conditions detailed in Table 1 with a sampling rate of 100 Hz. Due to high values in correlation (>80%) and signal-to-noise ratio (>15 dB), velocity measurements were conducted for at least 60 s per point at an accuracy of 0.001 m/s. To evaluate the stability of these measurements, a block-average analysis was performed on the flow measurements in flume G1, recorded for more than 60 s. The measurement data were divided into consecutive blocks of increasing size, the mean value was computed for each block and normalized by the total mean. As shown in Fig. 14, the block average converges toward the total mean as more data points are included into the blocks, stabilizing within less than 1% deviation from the total mean before completing 60 s of measurement. This confirms the consistency and reliability of the collected data within the chosen measurement period.

Small nonuniformities can be identified in the flow fields of the approach flow measured upstream of the bridge structures between

flumes G1, B1, and N1 in Fig. 13. In flume G1 at $Fr_0 = 0.28$ and $h_0 = 27$ cm, flow velocities ranged between 0.4 and 0.6 m/s with a standard deviation of 4% and the highest flow rates in the center of the flume. In flume B1 during series 3, the lowest flow velocities occurred in the lower right corner of the approach flow, only reaching 0.23 m/s. The observed standard deviation for the flow velocities is at 8% across the flow field. In flume N1 at $Fr_0 = 0.15$, flow velocities varied between 0.19 and 0.26 m/s and their standard deviation amounts to 2%. Comparing all three approach flows, the flow field in flume B1 appears slightly less symmetric and less homogenous with a larger amplitude variation.

Data Availability Statement

All data that support the findings of this study are available from the corresponding author upon reasonable request.

Acknowledgments

This study was carried out in the EMfloodResilience project (EMR 228) within the context of Interreg V A Euregio MeuseRhine and was 90% funded from the European Regional Development Fund. We thank our students Florence Dütz, Fabrice Hamonou, Gianni Massin, Milly Peyrard, Lino Schröter, Louisa Blitz, Ben Lindner, Mariia Gimelbrant, Dennis Ronkers, Michiel Hendriks, Ningyi Chen, and Ruben Wessendorp and all laboratory technicians for their assistance in the experimental modeling. Further, we gratefully acknowledge the reviewers and editors for their constructive comments and suggestions, which have contributed to improving the quality of this manuscript.

Author Contributions

Lisa Burghardt: Conceptualization; Data curation; Formal analysis; Investigation; Methodology; Validation; Visualization; Writing – original draft; Writing – review and editing. Daan Willem Poppema: Conceptualization; Data curation; Formal analysis; Investigation; Methodology; Validation; Visualization; Writing – review and editing. Loïc Bénet: Data curation; Formal analysis; Investigation; Methodology. Sébastien Erpicum: Conceptualization; Data curation; Funding acquisition; Methodology; Project administration; Supervision; Writing – review and editing. Davide Wüthrich: Conceptualization; Funding acquisition; Methodology; Project administration; Supervision; Writing – review and editing. Elena-Maria Klopries: Conceptualization; Funding acquisition; Project administration; Supervision; Validation; Writing – review and editing.

References

Schmocker, L., et al. 2016. *Schwemmholz an Hochwasserentlastungsanlagen von Talsperren*. München, Germany: Technische Universität München.

Bayón, A., D. Valero, and M. J. Franca. 2024. "Urban flood drifters (UFD): Identification, classification and characterisation." *J. Flood Risk Manage.* 17 (3): e13002. https://doi.org/10.1111/jfr3.13002.

Bénet, L., G. De Cesare, and M. Pfister. 2021. "Reservoir level rise under extreme driftwood blockage at ogee crest." *J. Hydraul. Eng.* 147 (1): 04020086. https://doi.org/10.1061/(ASCE)HY.1943-7900.0001818.

Bezzola, G. R., S. Gantenbein, R. Hollenstein, and H.-E. Minor. 2002. "Verklausung von Brückenquerschnitten." In *Moderne Methoden und Konzepte im Wasserbau*, edited by H.-E. Minor, 87–97. Zürich, Switzerland: Eidgenössische Technische Hochschule Zürich.

Burghardt, L., E.-M. Klopries, and H. Schüttrumpf. 2024a. "Structural damage, clogging, collapsing: Analysis of the bridge damage at the rivers Ahr, Inde and Vicht caused by the flood of 2021." *J. Flood Risk Manage.* 18 (1): e13001. https://doi.org/10.1111/jfr3.13001.

Burghardt, L., D. W. Poppema, L. Bénet, D. Wüthrich, S. Erpicum, and E.-M. Klopries. 2024b. *Multi-lab investigation of the effect of debris composition on bridge clogging during floods*. Zürich, Switzerland: Eidgenössische Technische Hochschule Zürich. https://doi.org/10.3929/ETHZ-B-000676025.

Cantero-Chinchilla, F. N., G. A. M. de Almeida, and C. Manes. 2021. "Temporal evolution of clear-water local scour at bridge piers with flow-dependent debris accumulations." *J. Hydraul. Eng.* 147 (10): 06021013. https://doi.org/10.1061/(ASCE)HY.1943-7900.0001920.

Chowdhury, P., I.-J. Fredericks, J. C. Alvarez, M. Clark, R. Jayaratne, J. J. Wijetunge, A. Raby, and P. Taylor. 2024. "Mixed debris interaction with obstacle array under extreme flood conditions." *J. Flood Risk Manage.* 17 (3): e12987. https://doi.org/10.1111/jfr3.12987.

de Cicco, P. N., E. Paris, L. Solari, and V. Ruiz-Villanueva. 2020. "Bridge pier shape influence on wood accumulation: Outcomes from flume experiments and numerical modeling." *J. Flood Risk Manage.* 13 (2): e12599. https://doi.org/10.1111/jfr3.12599.

Diehl, T. H. 1997. *Potential drift accumulation at bridges*. Rep. No. FHWA-RD-97-028. Washington, DC: Federal Highway Administration.

Erpicum, S., D. Poppema, L. Burghardt, L. Benet, D. Wüthrich, E.-M. Klopries, and B. Dewals. 2024. "A dataset of floating debris accumulation at bridges after July 2021 flood in Germany and Belgium." *Sci. Data* 11 (1): 1092. https://doi.org/10.1038/s41597-024-03907-8.

Follett, E., I. Schalko, and H. Nepf. 2020. "Momentum and energy predict the backwater rise generated by a large wood jam." *Geophys. Res. Lett.* 47 (17): e2020GL089346. https://doi.org/10.1029/2020GL089346.

Franca, M., D. Valero, A. Bayon, E. Martínez-Gomariz, and B. Russo. 2024. "October 2024 floods in the Valencia region, Eastern Spain: One example too many of hazardous debris." Accessed November 6, 2024. https://blogs.egu.eu/divisions/hs/2024/11/06/floods-valencia-hazardous-debris/.

Friedrich, H., D. Ravazzolo, V. Ruiz-Villanueva, I. Schalko, G. Spreitzer, J. Tunnicliffe, and V. Weitbrecht. 2022. "Physical modelling of large wood (LW) processes relevant for river management: Perspectives from New Zealand and Switzerland." *Earth Surf. Processes Landforms* 47 (1): 32–57. https://doi.org/10.1002/esp.5181.

Furlan, P. 2019. "Blocking probability of large wood and resulting head increase at ogee crest spillways." Doctoral dissertation, École Polytechnique Fédérale de Lausanne, Instituto Superior Técnico da Universidade de Lisboa.

Furlan, P., M. Pfister, J. Matos, C. Amado, and A. J. Schleiss. 2019. "Experimental repetitions and blockage of large stems at ogee crested spillways with piers." *J. Hydraul. Res*. 57 (2): 250–262. https://doi.org/10.1080/00221686.2018.1478897.

Gschnitzer, T., B. Gems, B. Mazzorana, and M. Aufleger. 2017. "Towards a robust assessment of bridge clogging processes in flood risk management." *Geomorphology* 279 (Feb): 128–140. https://doi.org/10.1016/j.geomorph.2016.11.002.

Hartlieb, A. 2015. *Schwemmholz in Fließgewässern: Gefahren und Lösungsmöglichkeiten*. München, Germany: Technical Univ. of Munich.

Innocenti, L., et al. 2025. "Formation of wood obstructions at bridges: Processes, related problems, and prediction tools." *Int. J. Bridge Eng. Manage. Res.* 2 (1): 21425002. https://doi.org/10.70465/ber.v2i1.12.

Koks, E. E., K. C. H. van Ginkel, M. J. E. van Marle, and A. Lemnitzer. 2022. "Brief communication: Critical infrastructure impacts of the 2021 mid-July western European flood event." *Nat. Hazards Earth Syst. Sci.* 22 (12): 3831–3838. https://doi.org/10.5194/nhess-22-3831-2022.

Lambert, S., F. Bourrier, A. R. Ceron-Mayo, L. Dugelas, F. Dubois, and G. Piton. 2023. "Small-scale modeling of flexible barriers. I: Mechanical similitude of the structure." *J. Hydraul. Eng.* 149 (3): 04022043. https://doi.org/10.1061/JHEND8.HYENG-13070.

Landesamt für Umwelt Rheinland-Pfalz. 2022. "Bericht: Hochwasser im Juli 2021." Accessed February 4, 2025. https://lfu.rlp.de/bevoelkerung/aktuelles/bericht-zum-hochwasser-im-juli-2021-veroeffentlicht_upload/pdf/Hochwasser_im_Juli2021.pdf.

This work is made available under the terms of the Creative Commons Attribution 4.0 International license.

Lange, D., and G. R. Bezzola. 2006. "Schwemmholz: Probleme und Lösungsansätze." Accessed November 30, 2023. https://ethz.ch/content/dam/ethz/special-interest/baug/vaw/vaw-dam/documents/das-institut/mitteilungen/2000-2009/188.pdf.

Lehmkuhl, F., H. Schüttrumpf, J. Schwarzbauer, C. Brüll, M. Dietze, P. Letmathe, C. Völker, and H. Hollert. 2022. "Assessment of the 2021 summer flood in Central Europe." *Environ. Sci. Eur.* 34 (Oct): 107. https://doi.org/10.1186/s12302-022-00685-1.

Lyn, D., T. Cooper, and Y.-K. Yi. 2003. *Debris accumulation at bridge crossings: Laboratory and field studies*. West Lafayette, IN: Purdue Univ. https://doi.org/10.5703/1288284313171.

Majtan, E., L. S. Cunningham, and B. D. Rogers. 2024. "Riverine flow and floating wooden debris interaction with an arch bridge: Flume experiments." *J. Hydraul. Res.* 62 (6): 542–559. https://doi.org/10.1080/00221686.2024.2437688.

Martín-Vide, J. P., et al. 2023. "Large wood debris that clogged bridges followed by a sudden release: The 2019 flash flood in Catalonia." *J. Hydrol.: Reg. Stud.* 47 (Jun): 101348. https://doi.org/10.1016/j.ejrh.2023.101348.

Mohr, S., et al. 2023. "A multi-disciplinary analysis of the exceptional flood event of July 2021 in central Europe. Part 1: Event description and analysis." *Nat. Hazards Earth Syst. Sci.* 23 (2): 525–551. https://doi.org/10.5194/nhess-23-525-2023.

Okamoto, T., H. Takebayashi, M. Sanjou, R. Suzuki, and K. Toda. 2020. "Log jam formation at bridges and the effect on floodplain flow: A flume experiment." Supplement, *J. Flood Risk Manage.* 13 (S1): e12562. https://doi.org/10.1111/jfr3.12562.

Okamoto, T., K. Tanaka, K. Matsumoto, and T. Someya. 2021. "Influence of velocity field on driftwood accumulation at a bridge with a single pier." *Environ. Fluid Mech.* 21 (3): 693–711. https://doi.org/10.1007/s10652-021-09793-7.

Panici, D., and G. A. M. de Almeida. 2018. "Formation, growth, and failure of debris jams at bridge piers." *Water Resour. Res.* 54 (9): 6226–6241. https://doi.org/10.1029/2017WR022177.

Panici, D., and G. A. M. de Almeida. 2020. "Influence of pier geometry and debris characteristics on wood debris accumulations at bridge piers." *J. Hydraul. Eng.* 146 (6): 04020041. https://doi.org/10.1061/(ASCE)HY.1943-7900.0001757.

Panici, D., and P. Kripakaran. 2021. "Trapping large wood debris in rivers: Experimental study of novel debris retention system." *J. Hydraul. Eng.* 147 (3): 04020101. https://doi.org/10.1061/(ASCE)HY.1943-7900.0001859.

Parola, A. C., C. J. Apelt, and M. A. Jempson. 2000. *Debris forces on highway bridges*. Washington, DC: Transportation Research Board.

Piton, G., A. R. Ceron-Mayo, and S. Lambert. 2023. "Small-scale modeling of flexible barriers. II: Interactions with large wood." *J. Hydraul. Eng.* 149 (3): 04022044. https://doi.org/10.1061/JHEND8.HYENG-13071.

Poppema, D. W., L. Burghardt, L. Benet, D. Wüthrich, E.-M. Klopries, B. Dewals, and S. Erpicum. 2025. "Bridge clogging in Belgium and Germany during the 2021 floods." *Water Resour. Res.* 61 (11): e2024WR039218. https://doi.org/10.1029/2024WR039218.

Poppema, D. W., and D. Wüthrich. 2024. "Comment on 'Momentum and energy predict the backwater rise generated by a large wood jam' by Follett, E., Schalko, I. and Nepf, H." *Geophys. Res. Lett.* 51 (8): e2023GL106348. https://doi.org/10.1029/2023GL106348.

Rickli, C., A. Badoux, D. Rickenmann, N. Steeb, and P. Waldner. 2018. "Large wood potential, piece characteristics, and flood effects in Swiss mountain streams." *Phys. Geogr.* 39 (6): 1–23. https://doi.org/10.1080/02723646.2018.1456310.

Ronckers, D., D. W. Poppema, and D. Wüthrich. 2024. "Experimental study on driftwood accumulation at submerged culverts." In *Proc., 10th Int. Symp. on Hydraulic Structures*. Zürich, Switzerland: Eidgenössische Technische Hochschule Zurich. https://doi.org/10.3929/ethz-b-000676024.

Ruiz-Villanueva, V., J. M. Bodoque, A. Díez-Herrero, and E. Bladé. 2014. "Large wood transport as significant influence on flood risk in a mountain village." *Nat. Hazards* 74 (2): 967–987. https://doi.org/10.1007/s11069-014-1222-4.

Schalko, I. 2018. "Modeling hazards related to large wood in rivers." Doctoral thesis, Laboratory of Hydraulics, Hydrology and Glaciology, Eidgenössische Technische Hochschule Zurich.

Schalko, I., C. Lageder, L. Schmocker, V. Weitbrecht, and R. M. Boes. 2019. "Laboratory flume experiments on the formation of spanwise large wood accumulations: I. Effect on backwater rise." *Water Resour. Res.* 55 (6): 4854–4870. https://doi.org/10.1029/2018WR024649.

Schmocker, L., and W. H. Hager. 2011. "Probability of drift blockage at bridge decks." *J. Hydraul. Eng.* 137 (4): 470–479. https://doi.org/10.1061/(ASCE)HY.1943-7900.0000319.

Schmocker, L., and W. H. Hager. 2013. "Scale modeling of wooden debris accumulation at a debris rack." *J. Hydraul. Eng.* 139 (8): 827–836. https://doi.org/10.1061/(ASCE)HY.1943-7900.0000714.

Schmocker, L., and V. Weitbrecht. 2013. "Driftwood: Risk analysis and engineering measures." *J. Hydraul. Eng.* 139 (7): 683–695. https://doi.org/10.1061/(ASCE)HY.1943-7900.0000728.

Soori, S., and H. Karami. 2024. "Laboratory study on relative energy loss and backwater rise at bridge piers and abutment." *Model. Earth Syst. Environ.* 10 (1): 1359–1373. https://doi.org/10.1007/s40808-023-01830-2.

Stolle, J., T. Takabatake, T. Mikami, T. Shibayama, N. Goseberg, I. Nistor, and E. Petriu. 2017. "Experimental investigation of debris-induced loading in tsunami-like flood events." *Geosciences* 7 (3): 74. https://doi.org/10.3390/geosciences7030074.

Tubaldi, E., et al. 2022. "Invited perspectives: Challenges and future directions in improving bridge flood resilience." *Nat. Hazards Earth Syst. Sci.* 22 (3): 795–812. https://doi.org/10.5194/nhess-22-795-2022.

Tullis, B. P., B. M. Crookston, and D. B. Bung. 2019. "Weir head-discharge relationships: A multi-lab exercise." In *Proc., 38th IAHR World Congress—Water: Connecting the World*, 486–500. Madrid, Spain: International Association for Hydro-Environment Engineering and Research. https://doi.org/10.3850/38WC092019-0806.

Wallerstein, N. P., C. V. Alonso, S. J. Bennett, and C. R. Thorne. 2001. "Distorted Froude-scaled flume analysis of large woody debris." *Earth Surf. Processes Landforms* 26 (12): 1265–1283. https://doi.org/10.1002/esp.271.

Welber, M., W. Bertoldi, and M. Tubino. 2013. "Wood dispersal in braided streams: Results from physical modeling." *Water Resour. Res.* 49 (11): 7388–7400. https://doi.org/10.1002/2013WR014046.

Wüthrich, D., P. A. Korswagen, H. Selvam, J. Oetjen, J. Bricker, and H. Schüttrumpf. 2025. "Field survey assessment of flood loads and related building damage from the July 2021 event in the Ahr Valley (Germany)." *J. Flood Risk Manage.* 18 (1):e13024. https://doi.org/10.1111/jfr3.13024.

Wüthrich, D., C. Ylla Arbós, M. Pfister, and A. J. Schleiss. 2020. "Effect of debris damming on wave-induced hydrodynamic loads against free-standing buildings with openings." *J. Waterway, Port, Coastal, Ocean Eng.* 146 (1): 04019036. https://doi.org/10.1061/(ASCE)WW.1943-5460.0000541.

Yan Toe, C., W. Uijttewaal, and D. Wüthrich. 2025. "Stability of an idealized floating carpet of plastic spheres in an open channel flow." *J. Hydraul. Eng.* 151 (4): 04025010. https://doi.org/10.1061/JHEND8.HYENG-14233.

This work is made available under the terms of the Creative Commons Attribution 4.0 International license.